

1 **A Universal Stress Protein upregulated by hypoxia may contribute to**
2 **chronic lung colonisation and intramacrophage survival in cystic fibrosis.**

3

4 Andrew O'Connor¹, Rita Berisio², Mary Lucey³, Kirsten Schaffer³, Siobhán McClean¹

5

6

7 1. School of Biomolecular and Biomedical Sciences, University College Dublin,
8 Belfield, Dublin 4, Ireland.

9 2. Institute of Biostructures and Bioimaging, National Research Council, Via
10 Mezzocannone 16, I-80134 Naples, Italy.

11 3. Department of Microbiology, St. Vincent's University Hospital, Elm Park, Dublin,
12 Ireland.

13

14 Running title: *Universal stress protein contributes to intramacrophage survival in cystic*
15 *fibrosis*

16 Corresponding author: Dr Siobhán McClean

17 Email: siobhan.mcclean@ucd.ie

18

19 **Keywords:** Respiratory infection, universal stress proteins; Cystic fibrosis, Adaptation;
20 Chronic infection; *Burkholderia cenocepacia*

21

22

23

24 **Summary:**

25

26 Universal stress proteins (USPs) are ubiquitously expressed in bacteria, plants and eukaryotes
27 and play a lead role in adaptation to environmental conditions. In Gram negative bacteria they
28 enable adaption of bacterial pathogens to the conditions encountered in the human niche,
29 including hypoxia, oxidative stress, osmotic stress, nutrient deficiency or acid stress, thereby
30 facilitating colonisation. We previously reported that all six USP proteins encoded within a
31 low-oxygen responsive locus in *Burkholderia cenocepacia* showed increased abundance
32 during chronic colonisation of the CF lung. However, the role of USPs in chronic infection is
33 not known. Using mutants derived from *B. cenocepacia* strain, K56-2, we show that USP76 is
34 required for growth and survival in many conditions associated with the CF lung including,
35 hypoxia, acidic conditions, oxidative stress. Moreover, it is involved in attachment to host
36 epithelial cells, but not virulence. It also has a role in survival in macrophages isolated from
37 people with CF. In contrast, another USP encoded in the same locus, USP92 had no effect on
38 host cell attachment or oxidative stress, but was responsible for a 3-fold increase in virulence.
39 Overall this shows that these USPs, both upregulated during chronic infection, have distinct
40 roles in *Burkholderia* pathogenesis and may support the survival of *B. cenocepacia* in the CF
41 lung. Specifically, USP76 is involved in its survival within CF macrophages, a hallmark of
42 *Burkholderia* infection.

43

44 **Introduction:**

45 Many opportunistic bacterial pathogens must adapt as they transition from their natural
46 environment to the host in order to survive within the host and establish an infection. Changes
47 in temperature, pH, osmolarity and oxygen availability are among the stresses that bacteria
48 must overcome as they move from their environmental niche to that of mammals. Universal
49 stress proteins (USPs) are expressed by bacteria and other microorganisms in response to a
50 wide variety of environmental conditions. They are extensively expressed throughout nature
51 from bacteria to archaea and eukaryotes but have not been identified in humans [1]. This breadth
52 of evolutionary range illustrates the importance of USPs in the resilience of organisms to
53 survive in stressful environments and while their role in bacterial cells is predominantly an
54 adaptive response to the changing environment, their contributions to bacterial pathogenesis
55 cover a range of different mechanisms [1]. In opportunistic pathogens such as *Mycobacterium*
56 *tuberculosis*, *Staphylococcus aureus* and *Pseudomonas aeruginosa*, USPs are involved in
57 survival within macrophages and low oxygen conditions [2-4], while an *Acinetobacter*
58 *baumannii* USP has a protective role against low pH and contributes to pathogenesis [5].
59 USPs were first identified in *E.coli* K-12 following exposure of cells to a variety of stresses,
60 heat shock, carbon and nitrogen starvation and ultraviolet radiation [6]. Expression of UspA in
61 *E. coli* was independent of the stringent stress response transcriptional activators RelA/SpoT,
62 RpoH, KatF, OmpR, AppY, Lrp, PhoB and H-NS [7]. *E. coli* *uspA* gene deletion mutants were
63 defective in survival over prolonged periods of growth under stress conditions such as induced
64 peroxide stress and osmotic shock [8]. *M. tuberculosis* USP Rv2623 contributes negatively to
65 virulence by regulating its growth in the transition to latency [4]. There are six *usp* genes in the
66 *E. coli* genome, while there are 10 *usp* genes encoded on the *M. tuberculosis* genome [1].
67 *Burkholderia cepacia* complex (Bcc) is a group of Gram negative bacteria that naturally occurs
68 in soil and in the rhizosphere of crop plants and causes chronic opportunistic life-threatening

69 infections in people with cystic fibrosis (CF) and immunocompromised patients. It can also
70 colonise pharmaceutical plants and contaminate pharmaceutical products and disinfectants [9].
71 It is highly antimicrobial resistant and once a chronic infection has been established,
72 eradication is rare. Its capacity to colonise diverse and harsh niches are exemplary and
73 consequently elucidation of its mechanisms of adaptation is essential. Sass *et al.* (2013)
74 identified a 50 gene locus which was dramatically upregulated under low oxygen conditions
75 and designated the low oxygen activated (lxa) locus [10]. We subsequently showed that 19
76 proteins encoded on the lxa locus showed increased abundance in late infection isolates from
77 chronically colonised CF patients [11]. These late chronic infection isolates also showed
78 increased attachment to CF lung epithelial cells [12]. Importantly, all six USPs encoded on the
79 lxa locus showed increased abundance with time of colonisation [11]. Among these lxa-
80 encoded *usp* genes, BCAM0276, encodes a UspA family stress protein which consistently
81 showed increased abundance in the later isolates from two chronically colonised patients and
82 was associated with increased gene expression [11]. Previously this USP (USP76) was reported
83 to be upregulated almost 60-fold in *B. cenocepacia* strain J2315 response to low oxygen [10]
84 and up to 40-fold in a comparative transcriptomic study of *B. contaminans* isolates from CF
85 patients [13]. There are 11 USPs in total encoded on the *B. cenocepacia* genome [14], ten of
86 which are on chromosome 2. The role of USP76 or other USPs in Bcc are unknown, but this
87 increased expression during chronic infection and under low oxygen conditions suggests that
88 this gene may be involved in chronic persistence of *Burkholderia cepacia* complex during
89 infection of the hypoxic CF lung. While USPs have been shown to protect bacteria from a
90 range of environmental pressures and stresses including extreme temperature changes,
91 antibiotic challenges, nutrient deprivation and oxidative stress, to date there are no published
92 data on the roles of USPs in chronic infection.

93 Limited oxygen is a hallmark of the CF lung due to rapid oxygen consumption by
94 microorganisms, invading neutrophils, impaired ventilation and contributions from mucous
95 plugs which together create an oxygen gradient within the lung [17]. These selective pressures
96 in CF airways drive adaptation in colonising bacteria, enabling them to overcome the various
97 microenvironments within the CF lung during infection. Furthermore, pathogens such as Bcc
98 can survive phagocytosis and even replicate within macrophage contributing to chronic
99 infection [18, 19]. We derived two Δusp deletion mutants and demonstrate that USPs such as
100 USP76 are at the forefront of this adaptation and may play a role in *B. cenocepacia*
101 pathogenesis. In addition, we compare it to another USP encoded on the *lxa* locus, which has
102 a comparable predicted size (table 1) and was also increased in abundance over time of chronic
103 infection and show the two USPs are distinct.

104

105 **Results:**

106 USP76 and USP92 both belong to the UspA protein family (PF00582) and contain single UspA
107 domain from residue 1 to 145. Both are predicted to exist as a homodimer formed largely by
108 the C-terminus of each monomer based on Swiss-Model ExPASy modelling (Figure. 1A), which
109 is common among other UspA molecules [20]. The BCAM0276 gene is the one of six USPs
110 encoded on the *lxa* locus. USP76 showed 6-fold increased abundance from early to late
111 infection in both sets of sequential isolates and was selected for detailed investigation.

112

113 **The $\Delta usp76$ mutant has a reduced attachment to host cells.** We previously showed that the
114 attachment of sequential *B. cenocepacia* isolates to CFBE41o⁻ cells increased over the time of
115 chronic infection [12]. Given the observed increase in BCAM0276 gene expression and
116 corresponding increase in USP76 protein abundance [11], the effect of the deletion of
117 BCAM0276 in *B. cenocepacia* strain K56-2 on attachment to cystic fibrosis epithelial cells,

118 CFBE41o⁻ was examined. The resulting $\Delta usp76$ mutant showed 90% reduced attachment to
119 CFBE41o⁻ cells ($p < 0.05$)(Figure 1b), which was restored to wildtype levels in the
120 $\Delta usp76_usp76$ complement strain. The reduction in attachment of the $\Delta usp76$ mutant was also
121 confirmed by confocal microscopy (a 6-fold reduction in attached $\Delta usp76$ mutant cells
122 compared to WT ($p < 0.05$, Figure 1 c and d)

123

124 **The $\Delta usp76$ mutant elicits reduced cytokine response but does not impact on acute**
125 **virulence.**

126 Given that deletion of the BCAM0276 gene resulted in reduced attachment to CFBE41o⁻ cells,
127 the secretion of IL-8 and IL-6 cytokines by CFBE41o⁻ cells was examined to investigate
128 whether there was a concomitant effect on cytokine secretion. IL-8 secretion was impaired in
129 response to the $\Delta usp76$ mutant strain (Figure 2a; $p = 0.0135$) while no statistically significant
130 effect on IL-6 relative to wild-type was observed. Despite the reduced IL-8 response of the
131 $\Delta usp76$ mutant, both the WT and the mutant strains were highly virulent, with 0% survival at
132 all dilutions of inoculum at 48 hours and consequently the LD₅₀ was determined at 24 hours
133 (Figure 2c). The $\Delta usp76$ mutant strain showed comparable virulence in the *G. mellonella* acute
134 virulence infection model.

135

136 **USP76 is required for survival in low oxygen and under an oxidative environment.**

137 Previous studies on bacterial USPs highlight roles in survival during challenging
138 environmental conditions [1], given the increase in BCAM0276 gene expression and in
139 abundance of USP76, the response of $\Delta usp76$ under various environmental pressures
140 experienced during chronic infection was examined. It has been shown that the *lxa* locus,
141 including the BCAM0276 gene, was dramatically upregulated in response to low oxygen [10]
142 therefore it was important to understand if USP76 was involved in survival in response to low

143 oxygen. The K56-2 strain was unable to grow in oxygen environments lower than 6% oxygen
144 and survival was considerably impaired at 6% oxygen (Figure 3). When exposed to 6% oxygen
145 in a controlled hypoxia chamber, no *Δusp76* mutant cells survived to day 8, indicating that this
146 gene is critical to survival under low oxygen. Complementation of the gene in the
147 *Δusp76_usp76* strain restored survival to near WT levels.

148

149 The CF lung is also characterised by constant inflammation and production of reactive oxygen
150 species (ROS) due to persistent bacterial infections. The impact of the oxidative environment
151 on the survival of the *Δusp76* mutant was examined using inorganic peroxide (H₂O₂) and
152 organic peroxide (tert-butyl hydroperoxide). Growth of the *Δusp76* mutant was impaired when
153 cultured in the presence of hydrogen peroxide (p = 0.0016, Figure 3b) although no significant
154 difference in growth was observed for tert-butyl hydroperoxide over a period of 20 hours
155 (Figure 3c, p = 0.2731).

156

157 **USP76 is required for growth and survival at acidic pH and survival in nutrient limited**
158 **conditions.**

159 A number of bacterial USPs allow survival under acidic conditions. Growth of the *Δusp76*
160 mutant in LB at low pH (pH 4.5) was reduced (p < 0.003) over 20 hours relative to WT when
161 normalised for growth in LB at physiological pH (~pH 7.4, Figure 4a). Growth of the
162 *Δusp76_usp76* complemented strain was comparable to WT levels. When the strains were
163 plated to determine the viable CFU remaining after exposure to acidic pH at a range of time
164 points, it was apparent that viability of the K56-2 strain following growth in acidic conditions
165 was also dependent on USP76 expression (Figure 4b), particularly after 2 hours exposure (p =
166 0.0092). The *Δusp76_usp76* complement strain initially showed impairment of viability, but
167 this recovered over time to reach WT levels within 5 hours of exposure to acidic pH.

168

169 The effect of deletion of the BCAM0276 gene on survival under long term nutrient limited
170 conditions was also examined over 28 days. All three strains showed reduced survival over the
171 first 3 days in glucose free medium, however both the WT and the $\Delta usp76_usp76$
172 complemented strains recovered within 5 days, reaching almost 100% survival within 20 days.
173 In contrast, the $\Delta usp76$ mutant strain did not recover to the same extent, reaching 50 % survival
174 by day 28 ($p = 0.0001$, Figure 4c).

175

176 **Impact of USP76 on cellular permeability and antibiotic susceptibility.**

177 The $\Delta usp76$ mutation had a moderate effect on cellular permeability as determined by the
178 uptake of the cell permeable Hoechst dye over a two-hour period ($p < 0.0001$; Figure S1). The
179 $\Delta usp76_usp76$ complement showed much higher fluorescent intensity than the WT and $\Delta usp76$
180 strains, possibly due to the deletion of the BCAL1674-1675 encoded efflux pump during the
181 complementation process, which resulted in greater accumulation of Hoechst 33324 dye. In
182 contrast to the alteration in cellular permeability, the BCAM0276 gene did not have any role
183 in survival in response to antibiotic challenges encountered during treatment for CF infection.
184 Growth following exposure to antibiotics with a range of mode of actions (Meropenem,
185 Levofloxacin, Ceftazidime and Polymyxin B) was comparable for the WT and the $\Delta usp76$
186 mutant strains ($p = 0.909$) (Figure S2, S3). The CF lung and the airway surface liquid also
187 represent high salt environments with 1% w/v NaCl concentrations reported for the ASL of
188 people with CF compared to 0.7% in healthy controls [21]. This creates osmotic stress on any
189 pathogens colonising the CF lung. Growth of the $\Delta usp76$ mutant was comparable to that of the
190 WT strain over a range of salt concentrations (0 to 5% NaCl, $p = 0.72$) indicating that USP76
191 does not play a role in the salt tolerance of *B. cenocepacia* (Figure S4).

192

193 **Deletion of *usp76* has no effect on mucoidy, motility or biofilm formation.**

194 Alterations in mucoid phenotype have been associated with chronically infecting Bcc isolates
195 [22], however, deletion of the *usp76* gene did not impact on EPS production when grown on
196 YEM agar plates in either normoxic or hypoxic conditions (Figure S5, Table S3). Motility was
197 comparable between the WT and the $\Delta usp76$ mutant strain (Figure S6). No statistically
198 significant differences were observed for motility phenotype when analysed by ANOVA,
199 swimming $p = 0.9720$, swarming $p = 0.2044$ and twitching $p = 0.4226$. In addition, the ability
200 for *B. cenocepacia* to form biofilms was not affected by the presence of the *usp76* gene (Figure
201 S7) under normal oxygen conditions or hypoxic conditions.

202

203 **USP76 is required for survival of *B. cenocepacia* in CF macrophages.**

204 Bcc can survive and replicate within macrophage [18] allowing the organism to evade both
205 host immune response and antibiotic treatments. Given that the pH of the intramacrophage
206 phagosome is estimated to be between 6.2 and 4.5, and that we have shown that the $\Delta usp76$
207 mutant is more susceptible to low pH and oxidative induced stress, we wanted to investigate
208 whether USP76 might contribute to the survival of *B. cenocepacia* inside macrophages. Firstly
209 we examined whether the intracellular uptake into the U397 macrophage-like cell line was
210 altered by the presence or absence of USP76 and found that there was a 60% reduction in the
211 number of the $\Delta usp76$ mutant cells that are internalised by the U937 line compared to WT
212 (Figure 5a, $p = 0.002$). Phagocytosis of the $\Delta usp76_usp76$ complement strain was equivalent
213 to that of WT. Survival of the $\Delta usp76$ mutant within U937 macrophages cells was also
214 significantly impaired at 24 h (Figure 5b, $p = 0.0378$). In contrast survival of the complemented
215 strain was restored to wild type levels. Acidification is impaired in CF macrophages due to the
216 dysfunctional CFTR, consequently, in order to examine whether this had relevance in the CF
217 context, we sought ethics approval to investigate the survival of the strains in PBMC-derived

218 macrophages from 12 people with CF. PBMC samples from five subjects could be successfully
219 differentiated to macrophage cells in sufficient numbers to be suitable for use in uptake and
220 intracellular assays. The uptake of the $\Delta usp76$ mutant strain by PBMC-derived macrophage
221 from two patients was significantly reduced (** $p = 0.0018$, *** $p = 0.0004$) when compared to
222 the WT strain. More importantly, intracellular survival of the $\Delta usp76$ mutant was assessed in
223 CF patient derived macrophage cells, and showed significantly reduced survival in four out of
224 five macrophage preparations (Figure 6b) ($0.05 < p > 0.0001$).

225

226 **The USPs encoded in the *lxa* Locus are not redundant.**

227 As previously mentioned there are six USPs encoded on the *lxa* locus, all of which showed
228 increased abundance in late stage isolates from chronically colonised people with CF. Having
229 characterised USP76, we wanted to examine whether other USPs expressed within the locus
230 share the same functions. We chose a *uspA* gene downstream of BCAM0276 as it was
231 upregulated by 201-fold in response to low oxygen and showed greatest increase in protein
232 abundance (up to 16 fold) in late stage isolates [10, 11]. A targeted single deletion mutant was
233 generated for the BCAM0292 gene; however, despite many attempts we were unable to
234 complement the strain with the BCAM0292 gene. Using the targeted deletion mutant, $\Delta usp92$,
235 the role of USP92 was characterised and compared with USP76. Consistent with $\Delta usp76$, the
236 $\Delta usp92$ mutant showed impaired growth under acidic conditions, relative to the WT strain K56-
237 2 (Figure 7, $p < 0.001$). But in contrast to the $\Delta usp76$ mutant, the $\Delta usp92$ mutant showed a
238 three-fold reduction in virulence as determined by LD₅₀ in *G. mellonella* larvae relative to the
239 WT strain ($p = 0.0228$, Figure 7). Moreover, the $\Delta usp92$ mutant showed slower growth in the
240 presence of high salt (Figure 7c $p < 0.001$) in contrast to $\Delta usp76$. USP92 may also confer slight
241 but significant protection against sucrose at 2.5% ($p = 0.04$) and 5% w/v sucrose ($p =$
242 0.005)(Figure S8a). Furthermore, the $\Delta usp92$ mutant also showed a slight but significantly

243 reduced uptake of the cell-permeable Hoechst dye ($p < 0.001$). In contrast to the $\Deltausp76$
244 mutant, no significant change in CBE41o⁻ cell attachment was observed in the $\Deltausp92$ mutant
245 compared with the WT strain (Figure S8b). Moreover, while USP76 seemed to be involved in
246 survival in response to oxidative stress, the USP92 does not, with the $\Deltausp92$ mutant showing
247 comparable growth in the presence of hydrogen peroxide (Figure S8c). Consistent with the
248 $\Deltausp76$ mutant, there was no alteration in EPS production in the $\Deltausp92$ mutant under
249 normoxic conditions when compared to the WT strain (Figure S9a) nor were there significant
250 difference in antibiotic susceptibility observed (Figure S9 b,c).

251

252 **Structural features of USP76 and USP92 explain their differential host cell attachment**
253 **abilities.**

254 To identify structural determinants responsible for the different behaviours of USP76 and
255 USP92, in particular their different abilities to bind to epithelial cells, we used homology
256 modelling and analysed resulting structures. Both structures are highly reliable, given the high
257 sequence identities with their template structures. The two protein structures share a similar
258 dimeric organisation (Figure 8), consistent with their relatively high sequence similarity
259 (sequence identity =41.8%). Each monomer is composed of an open-twisted, five-strand
260 parallel β -sheet, sandwiched by two α -helices on each side of the sheet ($\alpha1$ - $\alpha4$ in Figure 8) and
261 present structural features of ATP binding proteins. In both models, a wide ATP binding cleft
262 runs adjacent to the central β -sheet and contacts the α -helices $\alpha1$, $\alpha3$ and $\alpha4$ of each monomer
263 (Figure 8).

264 Strong differences between the two proteins are evident when electrostatic potential surfaces
265 are compared. Indeed, an overall negative electrostatic potential surface characterises USP92,
266 with only two positively charged patches due to Arg119-120 and Arg136 (Figure 9). Consistent
267 with a higher pI value of USP76 (pI=7.8) compared to USP92 (pI=5.0), the electrostatic

268 potential surface of USP76 presents several clusters of positively charged residues on the entire
269 surface of the protein, due mostly to arginine residues (Figure 9).

270

271 **Discussion:**

272 A hallmark of genus *Burkholderia* is its remarkable ability to survive and thrive in a range of
273 diverse environments, ranging from the soil, aquatic niches, disinfectants to the human host.

274 Its ability to adapt to changing environments contributes to its success as a human pathogen.

275 In this study we demonstrate that USPs support intramacrophage survival of *B. cenocepacia*
276 and consequently may play an important role in the chronic colonisation of *B. cenocepacia* in

277 people with cystic fibrosis. USPs are ubiquitous proteins which play a wide array of protective
278 roles in bacterial pathogens and appear to be central to pathogenesis of intracellular pathogens.

279 *B. cenocepacia* expresses 11 USPs. Six of these are encoded within the *lxa* locus, all of which
280 increase in abundance in chronic infection and show increased expression in response to low

281 oxygen [10, 11]. Despite the upregulation in response to low oxygen and chronic infection, we

282 now show that USP76 and USP92 have quite distinct roles in *B. cenocepacia*, highlighting a

283 clear lack of redundancy in these USPs. Moreover, we have shown that USP76, in particular,

284 is likely to be important for survival of *B. cenocepacia* in CF macrophage, a significant

285 characteristic of this pathogen.

286 To elucidate the role that both USPs play in Bcc chronic infection, we examined a series
287 of phenotypes associated with environmental pressures experienced during chronic infection

288 or associated with Bcc virulence. The CF lung has profoundly low pO₂ due to a combination

289 of disease associated issues including mucous plugging, constant neutrophilic inflammation

290 and increased epithelial oxygen consumption [17, 26]. Oxidative stress in the CF lung

291 contributes to the cycle of inflammation and is an inherent feature of CF [27]. Four key

292 phenotypes relating to growth and/or survival under conditions typical of the CF lung were

293 significantly altered in the $\Delta usp76$ mutant compared to the wildtype strain: hypoxia, low pH,
294 induced oxidative stress and nutrient starvation. Therefore, it is clear that USP76 (but not
295 USP92) protects *B. cenocepacia* against oxidative stress. UspA gene deletion mutants in
296 *Listeria monocytogenes* also had impaired growth when exposed to oxidative stress [28].
297 Similarly, *E. coli* UspA and UspD mutants were more susceptible to oxidative and superoxide
298 stress [8, 29]. *L. monocytogenes* UspA mutants exposed to acidic stress were also previously
299 found to have reduced cellular growth, albeit at a lower pH (pH 2.5) than that used by us [28].
300 In addition, an *A. baumannii* UspA mutant was also shown more susceptible to low pH and
301 also oxidative stress [5]. Overexpression of a mycobacteria USP encoded by RV2624c
302 increased survival in hypoxic conditions [30].
303 Previous reports showing that a *L. monocytogenes* UspA protected against low pH, oxidative
304 stress and enhanced survival within murine macrophage [28], led us to evaluate whether USP76
305 also contributed to the survival of *B. cenocepacia* in macrophages, particularly given that
306 USP76 was also protective in oxidative stress and involved in host cell attachment, in contrast
307 to USP92. The impaired survival of the $\Delta usp76$ mutant in U937 macrophage cells and,
308 crucially, our finding that survival was significantly impaired in 80% of the CF-patient derived
309 macrophage samples confirms that USP76 confers a clear survival advantage to *B. cenocepacia*
310 inside macrophage cells. People with CF can have impaired macrophage function, which can
311 lead to altered phagocytosis and killing of bacteria [31], consequently the role of USP76 in
312 uptake and survival in CF-patient derived macrophages is particularly noteworthy. Given that
313 impaired survival of the $\Delta usp76$ was not evident in all CF-patient derived macrophages
314 samples, it is clear that host factors also play a role. The BCAM0276 gene was previously
315 shown to be upregulated when *B. cenocepacia* strain K56-2 was internalised in murine
316 macrophages [32]. This work now confirms that USP76 contributes to survival of *B.*
317 *cenocepacia* within the CF lung and also within the CF macrophage. Moreover, our previously

318 observed increase in abundance of USP76 in chronically colonised patients indicates that
319 USP76 is very likely to be a major player in facilitating the long-term survival of this pathogen
320 within macrophages of CF patients.

321 The role of USP92 is distinct from that of USP76, as the two proteins are involved in
322 determining different subsets of phenotypes (Table 2). Although both USPs protect the
323 bacterial cell from acidic stress, only USP92 has a role in growth in the presence of osmotic
324 stress. Moreover, we observe that USP92 is important for virulence in the acute larval infection
325 model, in contrast to USP76, albeit not involved in host-cell attachment. The protective role
326 against osmotic stress is critical in the context of CF airway surface liquid and may contribute
327 to protection of *B. cenocepacia* in CF sputum. USPs in other species, e.g. atypical *E. coli*, have
328 also been shown to be involved in salt tolerance [33].

329 Different roles for individual USPs expressed by a bacterial species have previously
330 been observed in *E. coli*. Opposing roles in attachment have previously been reported for
331 different USPs expressed in *E. coli*; with UspC and UspE mutants showing enhanced host cell
332 attachment and loss of motility while UspF and UspG mutants had reduced host cell attachment
333 and maintained cell motility [34]. Moreover, *E. coli* UspA and UspD were required for
334 protection against oxidative stress while UspC and UspE were not. In *B. cenocepacia* opposing
335 roles in membrane permeability were also observed for USP76 and USP92, with the $\Delta usp76$
336 mutant having reduced permeability while the $\Delta usp92$ mutant had increased permeability
337 relative to the WT strain. A role in permeability would not be expected for cytosolic proteins
338 that are expressed without signal peptides (likelihood of 0.0104) (SignalP-5.0). Yet the
339 responses to Hoechst indicates that both these USPs may interact with the cellular membrane.
340 The role of USP76 in host cell attachment strengthens this view. We have identified USPs,
341 including USP76, among many cytosolic proteins in the outer membrane vesicles (OMVs)

342 released from *B. cenocepacia* strain by proteomic analysis (unpublished data), and their
343 presence in OMVs may provide a mechanism by which USPs can impact on the cell surface.
344 As with USP76, *E.coli* USPs have also been linked to cell adhesion when mutants were
345 assessed by yeast agglutination, with mutants of UspC and UspE enhancing cellular
346 attachment, USPs F and G reducing in attachment [34]. The surface arginine residues on
347 USP76 are likely to be involved in electrostatic interactions with sulfonate and carboxylate
348 groups heparan sulphate, a negatively charged linear sulphated glycosaminoglycan (GAG) on
349 the surface of epithelial cells. Indeed, it is well established that interactions of heparan sulphate
350 with proteins are primarily driven by ion pair interactions mediated by surface regions rich in
351 lysines and/or arginines, as in the case of the HBHA protein of *M. tuberculosis* [23-25].
352 Interestingly, macrophage cells increase expression of heparan sulphate under chronic
353 inflammatory conditions, which would confer additional advantages on Bcc [36]. We speculate
354 that USP76 is released from *B. cenocepacia* in OMVs, coating the bacterium and enhancing
355 attachment to both macrophage and epithelial cells conferring a major advantage in its survival
356 in the CF lung and increasing colonisation fitness. OMV released by *Vibrio cholerae* play a
357 comparable role in surface adaptation in vivo [37], and this will hypothesis will need to be
358 evaluated in *B. cenocepacia*.

359 USPs are clearly critical for an environmental bacterium such as *Burkholderia* to cope
360 with the breadth of stressful conditions that it is exposed to in soil. However, it is now clear
361 that USPs also confer substantial advantages on opportunistic pathogens adapting to the niche
362 environment of the CF lung. In particular, USP76 is a major contributor to macrophage
363 survival, while USP92 may confer advantages in the extracellular milieu, such as in CF
364 sputum. Furthermore, the enhanced expression of both USPs over the course of chronic
365 infection indicates that they play a role in the adaptation to chronic infection and represent
366 interesting targets to overcome chronic colonisation.

367

368 **Experimental Procedures:**

369 **Bacterial Strains and Growth Conditions**

370 Strains and plasmids used in this study are listed in table S1. Bacteria were routinely grown at
371 37°C in Luria-Broth (LB) medium with orbital shaking (200 rpm) unless otherwise stated.
372 Antibiotics, when required, were added to reach final concentrations as follows: 50 µg/ml
373 trimethoprim for *E. coli* and 100 µg/ml for *B. cenocepacia* and 40 µg/ml kanamycin for *E. coli*.

374

375 **Mammalian Cell Culture**

376 Cystic fibrosis epithelial cells, CFBE41o⁻ which are homozygous for the ΔF508 mutation of
377 the CFTR gene were routinely cultured in collagen/fibronectin coated flasks as previously
378 described [12]. The U937 macrophage cells were maintained as a suspension culture in
379 complete RPMI medium (Sigma-Aldrich) supplemented with 1 mM sodium pyruvate, 10 mM
380 4-(2-hydroxyethyl)-1-piperazineethanesulfonic acid (HEPES) buffer (pH 7.0 – 7.6), 1 mg /100
381 units streptomycin / penicillin, 10 % (v/v) FBS and 5 g/L D-glucose. U937 cells were plated in
382 24-well plates and after 24 h were induced to differentiate by the addition of 15 ng/ml of
383 phorbol 12-myristate 13-acetate (PMA) for 24 hours in full RPMI medium.

384

385 **Construction of Δusp mutants and complementation.**

386 Targeted gene deletions of BCAM0276 or BCAM0292 in the *B. cenocepacia* strain K56-2
387 were performed as described [38]. The amplicons used to construct the mutagenic plasmid
388 were cloned into pGPI-SceI-2 digested with *EcoRI* and *NheI*, using triparental mating, followed
389 by biparental mating to introduce the I-SceI endonuclease. Screening was performed on the
390 resulting colonies from bi-parental mating to determine if successful gene deletion had taken
391 place. Trimethoprim sensitive colonies were screened for gene deletion using the US forward

392 DS reverse primers (Table S2) and mutants were sent for sequencing to confirm sequence
393 deletion and stocks in glycerol prepared. To complement *B. cenocepacia* K56-2 Δ BCAM0276,
394 wild-type BCAM0276 was amplified from *B. cenocepacia* K56-2 with the complementation
395 primer pair (Table S2), digested with the restriction enzymes *NdeI* and *XbaI* and ligated into
396 similarly digested pMH447 [39]. The complementation plasmid was introduced into the mutant
397 by conjugation. Once transferred into the target mutant strain the complementation vector
398 integrates into the genome at aminoglycoside efflux genes (*BCAL1674-BCAL1675*), due to
399 sequence homology between the vector and target genome [40]. As before, pDAI-Sce-I, was
400 then introduced resulting in the replacement of BCAL1674-1675 by BCAM0276. The
401 complementation of the BCAM0276 gene was confirmed by PCR and by phenotype analysis.
402 Following genetic manipulation of *B. cenocepacia* K56-2 strain during gene deletion and
403 subsequent complementation, the presence of the plasmid pC3 was confirmed using three sets
404 of primers designed for genes RepA, oriC and dopC. The pC3 plasmid is a non-essential
405 replicon of *B. cenocepacia* and encodes for a number of virulence factors [41], which can be
406 lost during genetic manipulation. PCR was performed on confirmed mutants and complements
407 using primers 3001/3002, 3003/3004 and 3005/3006.

408

409 **Bacterial attachment to human CF epithelial cells.**

410 CFBE410⁻ cells were seeded in wells of a 24-well plate at a density of 4×10^5 cells / well in
411 antibiotic free medium and incubated overnight. The cells were then washed three times with
412 PBS and the mid-logarithmic phase bacterial cultures (OD_{600nm} 0.6-0.8) were resuspended in
413 MEM and added to each well at a concentration of 2×10^7 CFU / well (MOI 50:1). The plates
414 were centrifuged at $252 \times g$ for 5 min and incubated for 30 min at 37°C, 5% CO₂ to allow for
415 bacterial adherence. Wells were then washed with PBS and lysis buffer (0.25 % Triton X-100
416 in PBS) added to each well for 20 min at RT. Cell lysates were plated onto LB agar in duplicate

417 and incubated at 37°C for 48 hours. Resulting colonies were counted and the CFU/ml
418 determined. For microscopic visualisation of attachment, CFBE41o⁻ cells were seeded in
419 chamber slides (LabTek™) and incubated with bacteria for 30 min and washed with PBS as
420 outlined above. CFBE41o⁻ cells and adherent bacterial cells were fixed using 3 % w/v PFA
421 (pH 7.2) for 10 min at RT, washed with PBS and blocked with 5 % BSA in PBS for one hour
422 at RT. Cells were then incubated with a rabbit anti-Bcc antibody (courtesy of Prof U. Sajjan)
423 in 1% BSA PBS overnight at 4°C. Cells were then washed with PBS and incubated with an
424 anti-rabbit FITC conjugated antibody for 1 hour at 4°C. Cells were then washed twice with
425 PBS for 5 min. Nuclei were counterstained with DAPI (VectaShield) and visualised using an
426 Olympus FV-1000 confocal microscope. Bacterial attachment was expressed as number of
427 bacteria per 100 cells in 10 randomly selected fields.

428

429 **Cytokine secretion by CFBE41o⁻ cells following infection with *B. cenocepacia* strains.**

430 CFBE41o⁻ cells were seeded at a density of 4×10^5 cells / well in a 24-well plate in antibiotic
431 medium for 24 hours followed by a further 24 hours in antibiotic and serum free medium prior
432 to infection with *B. cenocepacia*. Overnight cultures of each strain were added to fresh LB
433 medium and grown to an OD_{600nm} of between 0.4 – 0.8. Each strain (2×10^7 CFU / ml, MOI
434 50:1) in MEM was added to each well in duplicate and incubated for 24 hours at 37°C and 5%
435 CO₂, then centrifuged at 315 x g for 12 min and supernatants transferred to -80°C for storage
436 prior to assay. Interleukin-8 (IL-8) and IL-6 secretion was determined using OptEIA™ ELISA
437 kits (Becton Dickenson) according to manufacturer's instructions and the absorbance measured
438 at 450 nm and 570 nm on the Biotek Synergy H1 Multiplate reader.

439

440 **Bacterial uptake and survival in U937 macrophage cells.**

441 The internalisation of *B. cenocepacia* strains by U937 macrophages was determined as
442 previously described [42]. Briefly overnight cultures of each strain were transferred to fresh
443 LB broth and incubated until mid-logarithmic phase (OD_{600nm} of 0.6 – 0.8) and diluted to an
444 MOI of 5:1 (2.5×10^6 CFU / ml) in RPMI medium. U937 cells were seeded at 5×10^5 cells /
445 ml in a 24-well plate, differentiated with PMA, washed twice with PBS, and 1 ml of each
446 bacterial culture applied in duplicate. The CFU applied was confirmed by serial dilution of
447 aliquots in Ringer's and plating in duplicate. The 24-well plates were centrifuged at $1100 \times g$
448 for 5 min, incubated at $37^\circ C$, 5% CO_2 for two hours, before washing with PBS. Extracellular
449 bacteria were killed with amikacin/ceftazidime (1mg/ml each) for two hours at $37^\circ C$, 5% CO_2 .
450 Wells were then washed 5 times with sterile PBS before cells were lysed with 0.25% Triton X-
451 100 for 15 min and scraped, diluted and plated as outlined above. To examine intracellular
452 survival of *B. cenocepacia* in U937 macrophage, bacteria were incubated with U937 as
453 described above and after two hours incubation with each strain, the wells were washed PBS
454 before addition of RPMI amikacin/ ceftazidime (1 mg/ml each) to each well and incubation
455 for a further 2 hours at $37^\circ C$, 5% CO_2 . The wells were subsequently washed twice with PBS
456 and fresh antibiotics replaced and incubated at $37^\circ C$, 5% CO_2 for various time points. Cells
457 were then washed, lysed, diluted and plated as described above and CFU determined after 48
458 h. The % survival was calculated as the intracellular CFU/ml at each time point relative to the
459 starting CFU/ml at time zero.

460

461 **Isolation of human peripheral mononuclear cells (PBMC) and differentiation**

462 Ethical approval was obtained from the St Vincent's University Hospital Research Ethics
463 committee. Age and gender matched adults with CF with no history of Bcc infection were
464 recruited from St Vincent's University Hospital and blood samples were collected in EDTA
465 tubes and diluted with the same volume of Dulbecco's PBS (DPBS) and mixed by inversion.

466 PBMCs were isolated by layering the blood over using Ficoll-Paque plus (GE Healthcare) and
467 centrifuging at 400 x g for 30 min at room temperature without braking. Upper layers
468 containing plasma and platelets were removed and the layers containing mononuclear cells
469 were transferred to a fresh tube containing three volumes of DPBS. Cells were centrifuged at
470 400 x g for 15 min at room temperature, resuspended in 8 ml DPBS and centrifuged at 100 x g
471 for 10 min at to remove platelets. The cells were resuspended in RPMI, cryopreserved at 2 x
472 10⁶ cells per ml in 40% FBS, 10% DMSO, 50% RPMI (v/v) and stored in liquid nitrogen.
473 Stored vials were revived as required and added to 5 ml RPMI 1640 (Sigma) medium (with no
474 additives) and centrifuged at 100 x g for 15 min. The pellets were resuspended in 5 ml of RPMI
475 1640, transferred to a T25 and incubated at 37°C, 5% CO₂ for two hours to allow the PBMCs
476 to adhere to the flask. The cells were washed four times with warmed Mg⁺⁺ and Ca⁺⁺ free
477 Dulbecco's PBS. Full RPMI 1640 medium containing 10 % autologous Human Serum
478 (Sigma), 10 mM HEPES (pH 7.0 – 7.6), 1mg / 100 units Penicillin / Streptomycin, 4.5 g/L D-
479 glucose, 1 mM sodium pyruvate and 1 X non-essential amino acids (Sigma) were added to the
480 flasks and the cells incubated with macrophage colony-stimulating factor (25 ng/ml, MC-
481 SF)(MSC) at 37°C, 5% CO₂ for 7 days with half media changes every 3 days. The cells were
482 harvested from the T25 flask by addition of porcine trypsin / EDTA (Sigma) in PBS and
483 incubated at 37°C for 20 min. Cells were gently removed from the flask with a cell scraper and
484 added to full RPMI medium and centrifuged at 252 x g for 10 min. Cells were resuspended in
485 1 ml of full RPMI medium, counted and diluted to the required concentration of cells in a 24-
486 well plate. Plates were then incubated for 24 hours at 37°C prior use. Bacterial uptake and
487 survival were then determined in the monocyte-derived macrophage cells as described for
488 U937 cells.

489

490 ***Galleria mellonella* acute infection model.**

491 To determine the acute virulence of the bacterial strains, the *Galleria mellonella* wax moth
492 larvae (Livefoods direct, Sheffield UK) were maintained at 15°C for seven days post-delivery
493 prior to use and used within 4 weeks [43]. Overnight cultures of each bacterial strain were
494 inoculated into 100 ml LB and grown to mid-logarithmic phase (OD_{600nm} of 0.6-0.8), diluted
495 to ~ 1 x 10⁶ CFU / ml and centrifuged at 2500 x g for 10 min. Pellets were resuspended in 2 ml
496 PBS and serially diluted to 10⁻⁷ in PBS and an aliquot of 20 µl of each dilution was injected
497 into the hindmost left proleg of 10 healthy larvae weighing between 0.2 and 0.4 g using a sterile
498 terumo 0.3 ml syringe. The bioburden injected was confirmed by serial dilution and plating.
499 The larvae were then incubated at 37°C and the % survival of the larvae determined over 72h
500 and plotted against the CFU bioburden inoculated value to calculate the LD₅₀ value for each
501 strain.

502

503 **Assessment of environmental stress responses**

504 A number of environmental stresses experienced during chronic infection within the CF lung
505 and macrophage environment were tested on each of the *B. cenocepacia* strains.

506 Controlled Hypoxia at 6% O₂: LB was equilibrated in a controlled hypoxia chamber (Coy
507 Laboratories) at 6% oxygen for 24h. Overnight cultures of the bacterial strains (10 ml) were
508 centrifuged at 4000 x g for 15 min, resuspended in 10 ml fresh LB, transferred to 40 ml hypoxia
509 equilibrated LB in 100 ml conical flask, and incubated statically at 37°C and 6 % O₂. Aliquots
510 were sampled at 24 hour intervals over 8 days, serially diluted to 10⁻⁷ in Ringer's solution,
511 plated onto LB agar plates in duplicate and then incubated at 37°C for 48 hours in normoxic
512 conditions before enumeration.

513 Low pH: Overnight cultures were diluted 1:100 LB broth at either pH 4.5 or standard pH ~7.5
514 and 300 µl aliquots added in duplicate to the wells of a 96-well round bottomed plate. The
515 plates were incubated at 37°C, with orbital shaking and OD_{600nm} measured every 15 min for 24

516 hours. Cell viability in low pH was also determined by inoculating a 100 ml flask of LB broth
517 at pH 4.5 with 10 ml of an overnight culture and incubated at 37°C, 170 rpm and plating hourly
518 samples as described previously.

519 High osmolarity: The effect of high osmolarity was determined in each *B. cenocepacia* strain
520 by adding 300 µl of a range of concentrations of NaCl (0 – 5% w/v) or sucrose (0 – 50%) to
521 rows of a 96-well plate. Overnight cultures were added to each well (3 µl) in duplicate and the
522 plates were incubated in a Biotek Synergy H1 multiplate reader at 37°C for 24 hours with
523 OD_{600nm} measured every 15 min.

524 Oxidative Stress: The effects of oxidative stress on the *B. cenocepacia* strains was assessed
525 firstly by exposing the strains to a series of concentrations of organic peroxide (*tert*-butyl
526 hydroperoxide) and inorganic peroxide (hydrogen peroxide, H₂O₂). Overnight cultures of each
527 strain were diluted 1:100 in fresh LB broth and 270 µl added in duplicate to corresponding
528 wells in a 96-well plate. A series of concentrations of either H₂O₂ (0 – 1 mM) or *tert*-butyl
529 hydroperoxide (0 – 200 µM) were added to the wells and growth determined in a Syngery H1
530 microplate reader at 37°C at medium shaking and OD_{600nm} measured every 15 min for 20 hours.
531 Viability of bacterial cells in an oxidative stress environment was also examined by treating
532 cultures with 700 µM H₂O₂ and incubated at 37°C, 200 rpm. Hourly samples were serially
533 diluted in Ringer's solution, and plated in duplicate to determine CFU / ml.

534 Heat Stress at 42°C: The effect of heat on each *B. cenocepacia* strain was determined by
535 transferring 10 ml of overnight cultures of each strain into 100 ml of pre-warmed (42°C) LB
536 and incubation at 42°C, 200 rpm. Hourly samples were diluted in Ringer's solution, plated and
537 enumerated after 48h.

538 Long term Nutrient Starvation: Long term nutrient starvation on each *B. cenocepacia* strain
539 was assessed as per Silva *et al* (2013). Overnight cultures of each strain grown in LB broth
540 were centrifuged at 4000 x g for 5 min and pellets were washed twice in 0.9 % w/v NaCl and

541 resuspended in 9 ml of M63 medium (2 g/L ammonium sulphate, 13.6 g/L potassium
542 phosphate monobasic, 0.5 mg/L Iron (II) sulphate, 0.2 g/L Magnesium sulfate) with no carbon
543 source. This was then added to 41 ml M63 medium in a 100 ml conical flask and incubated at
544 37°C with agitation of 200 rpm. Aliquots were taken for 28 days, serially diluted in Ringer's
545 solution, plated and counted after 48h incubation.

546

547 **Assessment of cell permeability by Hoechst 33324**

548 The cellular permeability of each strain was assessed by diluting overnight cultures 1:10 in
549 fresh LB medium, incubating at 37°C, 200 rpm for 5 hours, centrifuging at 4,000 x g for 3 min
550 and resuspending in sterile PBS. Each strain was then diluted to an OD_{600nm} of 0.1 with sterile
551 PBS and 180 µl added to 8 replicate wells of a row in a black, fluorescence 96-well plate and
552 2.5 µM of Hoechst 33324 added [44]. The plates were incubated in a Biotek Synergy H1
553 Multiplate reader at 37°C, medium shaking and fluorescence was measured every minute for 2
554 hours at an excitation of 355 nm and an emission of 460 nm. The mean fluorescence of 8
555 replicate wells was calculated for each strain and normalised with the T₀ value.

556

557 **Homology modelling**

558 The homology model structures of BCAM0276 and BCAM0292 were obtained after
559 consensus-based sequence alignment using the HHpred tool. The best model template for
560 BCAM0276 was identified as the structure of the TeaD stress protein from the TRAP
561 transporter TeaABC of *Halomonas elongata* (PDB code 3hgm, seqid 34.3%). For BCAM0292,
562 the best template was the BupsA stress protein from *Burkholderia pseudomallei* (PDB code
563 4wny, seqid 69.2%). Using these alignments, the homology models were built using the
564 program MODELLER [45]. Electrostatic potential surfaces were computed using the program
565 Chimera [46].

566

567 **Statistical analysis:**

568 Statistical analysis of host cell attachment, cytokine secretion, CF macrophage uptake and
569 survival data was performed by one-way ANOVA using Prism software. Two-way ANOVA
570 was used to analyze growth in the presence of organic and inorganic peroxide, growth under
571 acidic conditions and nutrient limitation. Statistical analysis of virulence, survival at 8 days in
572 hypoxic conditions, endpoint OD₆₀₀ in acidic conditions, U937 internalisation were performed
573 using a student's t-test.

574

575 Assessment of antibiotic resistance, mucoidy, motility, biofilm formation was performed as
576 described in the Supplementary information.

577

578 **Acknowledgements:**

579 We are most grateful to Prof Umadevi Sajjan (University of Michigan) for the gift of the anti-
580 Bcc antibody. This research was supported by a President's Award from the Institute of
581 Technology Tallaght, Dublin and a Government of Ireland Postgraduate scholarship Award
582 (GOIPG/2017/788) from the Irish Research Council and EU COST Action BM1003:
583 "Microbial cell surface determinants of virulence as targets for new therapeutics in cystic
584 fibrosis for Short Term Scientific Missions".

585

586 **References:**

- 587 1. O'Connor A, McClean S. The Role of Universal Stress Proteins in Bacterial Infections. *Curr*
588 *Med Chem* **2017**; 24:3970-9.
- 589 2. Schreiber K, Boes N, Eschbach M, et al. Anaerobic survival of *Pseudomonas aeruginosa* by
590 pyruvate fermentation requires an Usp-type stress protein. *J Bacteriol* **2006**; 188:659-68.
- 591 3. Boes N, Schreiber K, Härtig E, Jaensch L, Schobert M. The *Pseudomonas aeruginosa*
592 universal stress protein PA4352 is essential for surviving anaerobic energy stress. *J Bacteriol*
593 **2006**; 188:6529-38.
- 594 4. Drumm JE, Mi K, Bilder P, et al. *Mycobacterium tuberculosis* universal stress protein
595 Rv2623 regulates bacillary growth by ATP-Binding: requirement for establishing chronic
596 persistent infection. *PLoS pathogens* **2009**; 5:e1000460.
- 597 5. Elhosseiny NM, Amin MA, Yassin AS, Attia AS. *Acinetobacter baumannii* universal stress
598 protein A plays a pivotal role in stress response and is essential for pneumonia and sepsis
599 pathogenesis. *Int J Med Microbiol* **2015**; 305:114-23.
- 600 6. Nyström T, Neidhardt FC. Effects of overproducing the universal stress protein, UspA, in
601 *Escherichia coli* K-12. *J Bacteriol* **1996**; 178:927-30.
- 602 7. Nyström T, Neidhardt FC. Cloning, mapping and nucleotide sequencing of a gene
603 encoding a universal stress protein in *Escherichia coli*. *Molecular microbiology* **1992**; 6:3187-
604 98.
- 605 8. Nyström T, Neidhardt FC. Expression and role of the universal stress protein, UspA, of
606 *Escherichia coli* during growth arrest. *Molecular microbiology* **1994**; 11:537-44.
- 607 9. Vanlaere E, Baldwin A, Gevers D, et al. Taxon K, a complex within the Burkholderia
608 cepacia complex, comprises at least two novel species, *Burkholderia contaminans* sp. nov.
609 and *Burkholderia lata* sp. nov. *Int J Syst Evol Microbiol* **2009**; 59:102-11.
- 610 10. Sass AM, Schmerk C, Agnoli K, et al. The unexpected discovery of a novel low-oxygen-
611 activated locus for the anoxic persistence of *Burkholderia cenocepacia*. *Isme J* **2013**; 7:1568-
612 81.
- 613 11. Cullen L, O'Connor A, McCormack S, et al. The involvement of the low-oxygen-activated
614 locus of *Burkholderia cenocepacia* in adaptation during cystic fibrosis infection. *Scientific*
615 *Reports* **2018**; 8:13386.
- 616 12. Cullen L, O'Connor A, Drevinek P, Schaffer K, McClean S. Sequential *Burkholderia*
617 *cenocepacia* Isolates from Siblings with Cystic Fibrosis Show Increased Lung Cell
618 Attachment. *American journal of respiratory and critical care medicine* **2017**; 195:832-5.
- 619 13. Nunvar J, Kalferstova L, Bloodworth RA, et al. Understanding the Pathogenicity of
620 *Burkholderia contaminans*, an Emerging Pathogen in Cystic Fibrosis. *PLoS One* **2016**;
621 11:e0160975.
- 622 14. Winsor GL, Khaira B, Van Rossum T, Lo R, Whiteside MD, Brinkman FS. The *Burkholderia*
623 Genome Database: facilitating flexible queries and comparative analyses. *Bioinformatics*
624 **2008**; 24:2803-4.
- 625 15. Elizur A, Cannon CL, Ferkol TW. Airway inflammation in cystic fibrosis. *Chest* **2008**;
626 133:489-95.
- 627 16. Roesch EA, Nichols DP, Chmiel JF. Inflammation in cystic fibrosis: An update. *Pediatr*
628 *Pulmonol* **2018**; 53:S30-S50.
- 629 17. Montgomery ST, Mall MA, Kicic A, Stick SM, Arest CF. Hypoxia and sterile inflammation
630 in cystic fibrosis airways: mechanisms and potential therapies. *Eur Respir J* **2017**; 49.

- 631 18. Martin DW, Mohr CD. Invasion and intracellular survival of *Burkholderia cepacia*.
632 *Infection and immunity* **2000**; 68:24-9.
- 633 19. Rosales-Reyes R, Aubert DF, Tolman JS, Amer AO, Valvano MA. *Burkholderia*
634 *cenoecepacia* type VI secretion system mediates escape of type II secreted proteins into the
635 cytoplasm of infected macrophages. *PLoS One* **2012**; 7:e41726.
- 636 20. Sousa MC, McKay DB. Structure of the universal stress protein of *Haemophilus*
637 *influenzae*. *Structure* **2001**; 9:1135-41.
- 638 21. Grandjean Lapierre S, Phelippeau M, Hakimi C, et al. Cystic fibrosis respiratory tract salt
639 concentration: An Exploratory Cohort Study. *Medicine (Baltimore)* **2017**; 96:e8423.
- 640 22. Zlosnik JE, Hird TJ, Fraenkel MC, Moreira LM, Henry DA, Speert DP. Differential mucoid
641 exopolysaccharide production by members of the *Burkholderia cepacia* complex. *J Clin*
642 *Microbiol* **2008**; 46:1470-3.
- 643 23. Esposito C, Cantisani M, D'Auria G, et al. Mapping key interactions in the dimerization
644 process of HBHA from *Mycobacterium tuberculosis*, insights into bacterial agglutination.
645 *FEBS Lett* **2012**; 586:659-67.
- 646 24. Esposito C, Marasco D, Delogu G, Pedone E, Berisio R. Heparin-binding hemagglutinin
647 HBHA from *Mycobacterium tuberculosis* affects actin polymerisation. *Biochem Biophys Res*
648 *Commun* **2011**; 410:339-44.
- 649 25. Joseph PRB, Sawant KV, Iwahara J, Garofalo RP, Desai UR, Rajarathnam K. Lysines and
650 Arginines play non-redundant roles in mediating chemokine-glycosaminoglycan
651 interactions. *Sci Rep* **2018**; 8:12289.
- 652 26. Mendelsohn L, Wijers C, Gupta R, Marozkina N, Li C, Gaston B. A novel, noninvasive
653 assay shows that distal airway oxygen tension is low in cystic fibrosis, but not in primary
654 ciliary dyskinesia. *Pediatr Pulmonol* **2019**; 54:27-32.
- 655 27. Scholte BJ, Horati H, Veltman M, et al. Oxidative stress and abnormal bioactive lipids in
656 early cystic fibrosis lung disease. *J Cyst Fibros* **2019**; 18:781-9.
- 657 28. Seifart Gomes C, Izar B, Pazan F, et al. Universal stress proteins are important for
658 oxidative and acid stress resistance and growth of *Listeria monocytogenes* EGD-e in vitro
659 and in vivo. *PLoS One* **2011**; 6:e24965.
- 660 29. Nachin L, Nannmark U, Nyström T. Differential roles of the universal stress proteins of
661 *Escherichia coli* in oxidative stress resistance, adhesion, and motility. *J Bacteriol* **2005**;
662 187:6265-72.
- 663 30. Jia Q, Hu X, Shi D, et al. Universal stress protein Rv2624c alters abundance of arginine
664 and enhances intracellular survival by ATP binding in mycobacteria. *Sci Rep* **2016**; 6:35462.
- 665 31. Leveque M, Le Trionnaire S, Del Porto P, Martin-Chouly C. The impact of impaired
666 macrophage functions in cystic fibrosis disease progression. *J Cyst Fibros* **2017**; 16:443-53.
- 667 32. Tolman JS, Valvano MA. Global changes in gene expression by the opportunistic
668 pathogen *Burkholderia cenoecepacia* in response to internalization by murine macrophages.
669 *BMC Genomics* **2012**; 13:63.
- 670 33. de Souza CS, Torres AG, Caravelli A, Silva A, Polatto JM, Piazza RM. Characterization of
671 the universal stress protein F from atypical enteropathogenic *Escherichia coli* and its
672 prevalence in Enterobacteriaceae. *Protein Sci* **2016**; 25:2142-51.
- 673 34. Nachin L, Nannmark U, Nystrom T. Differential roles of the universal stress proteins of
674 *Escherichia coli* in oxidative stress resistance, adhesion, and motility. *J Bacteriol* **2005**;
675 187:6265-72.

- 676 35. Huang TY, Irene D, Zulueta MM, et al. Structure of the Complex between a Heparan
677 Sulfate Octasaccharide and Mycobacterial Heparin-Binding Hemagglutinin. *Angew Chem Int*
678 *Ed Engl* **2017**; 56:4192-6.
- 679 36. Swart M, Troeberg L. Effect of Polarization and Chronic Inflammation on Macrophage
680 Expression of Heparan Sulfate Proteoglycans and Biosynthesis Enzymes. *J Histochem*
681 *Cytochem* **2018**:22155418798770.
- 682 37. Zingl FG, Kohl P, Cakar F, et al. Outer Membrane Vesiculation Facilitates Surface
683 Exchange and In Vivo Adaptation of *Vibrio cholerae*. *Cell Host Microbe* **2020**; 27:225-37 e8.
- 684 38. Flannagan RS, Linn T, Valvano MA. A system for the construction of targeted unmarked
685 gene deletions in the genus *Burkholderia*. *Environ Microbiol* **2008**; 10:1652-60.
- 686 39. Hamad MA, Di Lorenzo F, Molinaro A, Valvano MA. Aminoarabinose is essential for
687 lipopolysaccharide export and intrinsic antimicrobial peptide resistance in *Burkholderia*
688 *cenozoecia*(dagger). *Molecular microbiology* **2012**; 85:962-74.
- 689 40. Hamad MA, Skeldon AM, Valvano MA. Construction of aminoglycoside-sensitive
690 *Burkholderia cenozoecia* strains for use in studies of intracellular bacteria with the
691 gentamicin protection assay. *Appl Environ Microbiol* **2010**; 76:3170-6.
- 692 41. Agnoli K, Frauenknecht C, Freitag R, et al. The third replicon of members of the
693 *Burkholderia cepacia* Complex, plasmid pC3, plays a role in stress tolerance. *Appl Environ*
694 *Microbiol* **2014**; 80:1340-8.
- 695 42. McKeon S, McClean S, Callaghan M. Macrophage responses to CF pathogens: JNK MAP
696 kinase signaling by *Burkholderia cepacia* complex lipopolysaccharide. *FEMS Immunol Med*
697 *Microbiol* **2010**:DOI:10.1111/j.574-695X.2010.00712.x.
- 698 43. Costello A, Herbert G, Fabunmi L, et al. Virulence of an emerging respiratory pathogen,
699 genus *Pandora*, in vivo and its interactions with lung epithelial cells. *J Med Microbiol*
700 **2011**; 60:289-99.
- 701 44. Coldham NG, Webber M, Woodward MJ, Piddock LJ. A 96-well plate fluorescence assay
702 for assessment of cellular permeability and active efflux in *Salmonella enterica* serovar
703 *Typhimurium* and *Escherichia coli*. *J Antimicrob Chemother* **2010**; 65:1655-63.
- 704 45. Bitencourt-Ferreira G, de Azevedo WF, Jr. Homology Modeling of Protein Targets with
705 MODELLER. *Methods Mol Biol* **2019**; 2053:231-49.
- 706 46. Yang Z, Lasker K, Schneidman-Duhovny D, et al. UCSF Chimera, MODELLER, and IMP: an
707 integrated modeling system. *J Struct Biol* **2012**; 179:269-78.
- 708
- 709
- 710
- 711
- 712

713

714 **Tables and Figures**

715

716 **Table 1:** USPs encoded on the *lxa* locus in *B. cenocepacia* J2315

717

Gene	Predicted MW	Predicted pI	Subcellular Localisation (PSortb)
BCAM0276	17016.4	8.23	cytoplasmic
BCAM0290	16139.1	4.61	unknown
BCAM0291	30520.5	6.74	cytoplasmic
BCAM0292	17743.9	4.82	unknown
BCAM0294	30586.3	6.75	unknown
BCAM0319	33622.2	6.86	unknown

718 Data taken from Burkholderia Genome database (www.burkholderia.com) [14]

719

720

721

722

723 **Table 2.** Comparison of phenotypes in USP76 and USP92.

724

Phenotype	USP76	USP92
Growth and or survival in		
Low pH	+	+
Osmotic stress	-	+
Oxidative stress	+	-
Nutrient limitation	+	
Osmolarity		+
Hypoxia	+++	
Host cell attachment	+++	-
Cytokine secretion	+	
Virulence in <i>G. mellonella</i>	-	+
Membrane permeability	slight	Slight
Mucoidy	-	-

725

726

727

728 **Figure Legends:**

729

730 **Figure 1: Comparison of the bacterial attachment to CFBE41o⁻ cells measured by**
731 **microbiological plating at an MOI of 50:1. A)** Predicted structure of the USP76 homodimer
732 using Swiss-Model Expasy. **b)** Comparison of the attachment of WT K56-2 and the $\Delta usp76$
733 mutant to CFBE41o⁻ lung epithelial cells by (b) microbiological plating and (c & d) confocal
734 microscopy. **B)** Data represent the mean CFU / ml for each strain in three independent
735 experiments. Error bars represent the standard error of the mean. *Signifies a statistically
736 significant difference in attachment of the $\Delta usp76$ mutant as determined by one-way ANOVA,
737 $p = 0.0117$. **C)** Confocal microscopy images of the attachment of WT K56-2 and the $\Delta usp76$
738 mutant to CFBE41o⁻ cells at a MOI of 50:1. *B. cenocepacia* cells were labelled with a primary
739 anti-Bcc antibody and detected with a secondary FITC-conjugated antibody (green). CFBE
740 nuclei were counterstained with DAPI (blue). **D)** Data represents the mean number of bacteria
741 / 100 cells of CFBE41o⁻ per strain for 10 randomly selected fields of view in three independent
742 experiments. Error bars represent the standard error of the mean. * Signifies statistical
743 significance, using a t test to compare data from three independent experiments, * $p < 0.0001$.

744

745

746 **Figure 2: Effect of deletion of BCAM0276 on cytokine response and virulence. A & B)**
747 **IL-8 and IL-6 cytokine secretion from CFBE41o⁻ cells following infection with the WT, the**
748 **$\Delta usp76$ mutant, the $\Delta usp76_usp76$ complement strains or negative control (MEM only). Bars**
749 **represent the mean level of detected cytokine in triplicate measured in two independent**
750 **experiments. Error bars represent the standard deviation. Statistical analysis was performed**
751 **using one-way ANOVA, * $p = 0.0135$. C) LD₅₀ values for the WT and the $\Delta usp76$ mutant**
752 **strains in the *G. mellonella* acute infection model at 24 hours. Data represent the mean LD₅₀**
753 **from three independent experiments and error bars represent the standard error of the mean.**

754

755 **Fig 3: Effect of USP76 on survival or growth to environmental conditions. A)** Mean
756 percentage survival of the WT, the $\Delta usp76$ mutant and the $\Delta usp76_usp76$ complement strains
757 after 8 days incubation in 6% oxygen in a controlled hypoxia chamber determined in three
758 independent experiments. Error bars represent the standard error of the mean; * $p = 0.0258$. **B**
759 **& C)** Mean OD₆₀₀ values of the WT and $\Delta usp76$ mutant strains following incubation with a
760 range of concentrations of **B)** H₂O₂ or **C)** Tert-butyl hydroperoxide (0 - 1000 μ M) for 20 hours.
761 Data displayed was normalised relative to treatment-free control and represent duplicate values
762 of three independent experiments, ** $p=0.0016$.

763

764 **Figure 4: Growth and Survival of the $\Delta usp76$ mutant under induced pH 4.5 stress or**
765 **nutrient limiting conditions. A)** Mean normalised endpoint OD_{600nm} values for each strain
766 WT, the $\Delta usp76$ mutant and $\Delta usp76_usp76$ complement following incubation in pH 4.5 LB
767 versus LB medium at pH 7. Data represent the mean normalised absorbance from 3
768 independent experiments, and error bars represent the standard error. Statistical analysis was
769 performed by t test, ** $p = 0.0068$. **B)** Normalised survival (CFU/ml) over time for each strain
770 the $\Delta usp76$ mutant and the $\Delta usp76_usp76$ complement strains compared to T₀ following
771 incubation in LB pH 4.5. Data represent the mean normalised CFU/ml from 3 independent
772 experiments, error bars represent the standard error. Statistical analysis by two-way ANOVA,
773 ** $p = 0.0019$. **C)** Mean % survival of the WT, the $\Delta usp76$ mutant and the $\Delta usp76_usp76$
774 normalised to Day 0 of each respective strain following incubation in nutrient limiting medium
775 (glucose free) over the course of 28 days. Data represent the mean % survival of 2 independent
776 experiments. Statistical analysis performed by two-way ANOVA, $p = 0.0038$

777
778
779
780
781
782
783
784
785
786
787
788
789
790
791
792
793
794
795
796
797
798
799
800
801
802
803
804
805
806
807
808
809
810
811
812
813
814
815
816
817
818
819
820
821
822
823

Figure 5: Uptake and survival of WT, the $\Delta usp76$ mutant and the $\Delta usp76_usp76$ complement strains in U937 macrophage cells. A) Uptake of the WT, the $\Delta usp76$ mutant and the $\Delta usp76_usp76$ complement strains by differentiated U937 macrophage cells. Data represent the intracellular uptake of the individual strains as a % of bacterial cells applied in three independent experiments. Error bars represent the standard error of the mean. **Statistically significant difference relative to the WT as determined by student t-test, $p = 0.002$); b) Survival of the $\Delta usp76$ mutant and the $\Delta usp76_usp76$ complement strains in U937 macrophage cells over time. Data represent the mean \log_{10} of CFU/ml from three independent experiments; error bars represent the standard error of the mean. *Statistically significant difference relative to the WT determined by two-way ANOVA ($p = 0.0378$).

Figure 6: Uptake and survival of the WT, the $\Delta usp76$ mutant and the $\Delta usp76_usp76$ strains in PBMC-derived macrophage from people with CF. a) % uptake and b) 24 h survival of the WT (black), the $\Delta usp76$ mutant (grey bars) or the $\Delta usp76_usp76$ complement strain (grey patterned bars). The data represent the means of three independent experiments and error bars represent the standard error of each mean. Statistically significant difference relative to the WT as determined by one-way ANOVA (** $p = 0.0018$; *** $p = 0.0004$). b) Survival of the wild type, $\Delta usp76$ mutant and the $\Delta usp76_usp76$ complement strains in CF monocyte-derived macrophage cells. Normalised data represent the mean \log of CFU/ml from three independent experiments, relative to time zero. Error bars represent the standard error of the mean. Statistically significant difference between mutant and WT strains was determined by one-way ANOVA as follows: CF2: $p = 0.0403$; CF 11, $p = 0.0016$; CF 12 $p = 0.0025$; CF13, $p < 0.0001$.

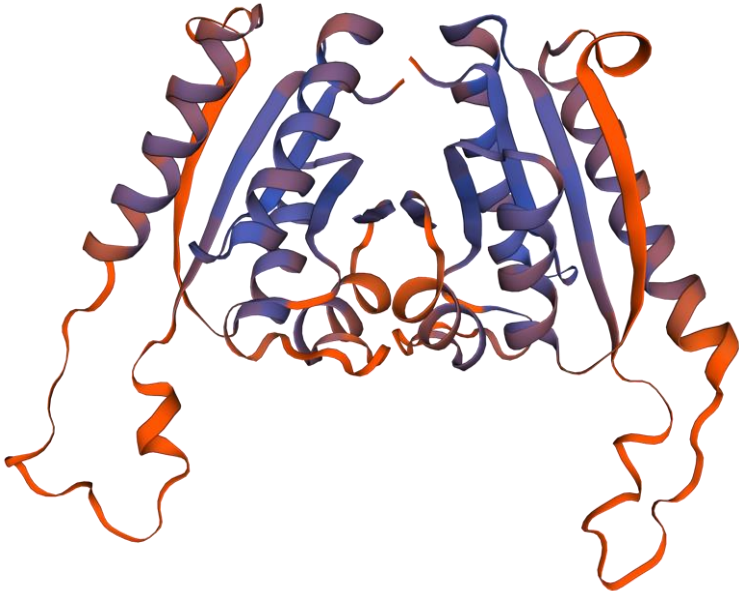
Figure 7: Phenotype analysis of USP92. A) Calculated LD_{50} values at 24 hours to determine virulence of the WT and the $\Delta usp92$ mutant strains in the *G. mellonella* wax moth larva model. Statistically significant difference relative to WT was determined by t-test, * $p = 0.0228$). B) Growth of WT and the $\Delta usp92$ mutant following incubation with LB broth at a pH of 4.5 for 20 hours as determined by OD_{600} . Data represent the mean OD values from three independent experiments at each timepoint. Error bars represent the standard error of the mean. Statistical significant difference determined by two-way ANOVA $p < 0.0001$. C) Mean endpoint absorbance values of WT and the $\Delta usp92$ mutant following incubation with concentrations of NaCl (0 – 5% w/v) for 24 hours at 37°C normalised to LB only. * $p = 0.003$ compared with wild type using two way ANOVA. D) Normalised fluorescence intensity data of the cellular uptake of Hoechst 33324 (excitation 355 nm, emission 460nm) in WT and the $\Delta usp92$ mutant over a period of two hours, incubated at 37°C. Data represents the mean of eight replicates of each strain, performed on two independent experiments (* $p < 0.001$, as determined by two way ANOVA)

Figure 8: Comparison of USP76 and USP92 protein structures. a) Cartoon and surface representations of the homology models of (a) USP76 and (b) USP92. The inset shows a detail of ATP binding mode. (c) Structure based sequence alignment as computed by DALI.

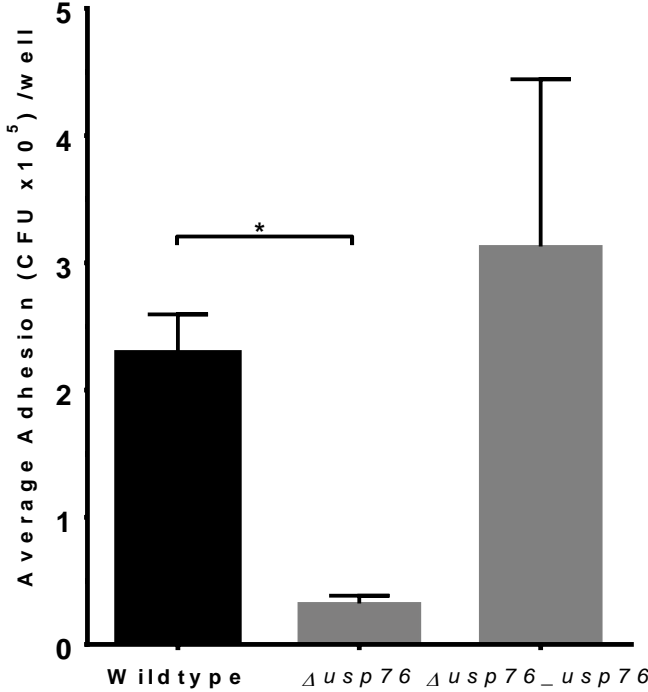
824 **Figure 9.** Side (left) and top (right) views of electrostatic potential surfaces of (a) USP76 and
825 (b) USP92; with red and blue denoting residues with negative and positive electrostatic
826 potential, respectively. The main residues contributing to the electrostatic potential are labelled.
827
828
829
830

Figure 1

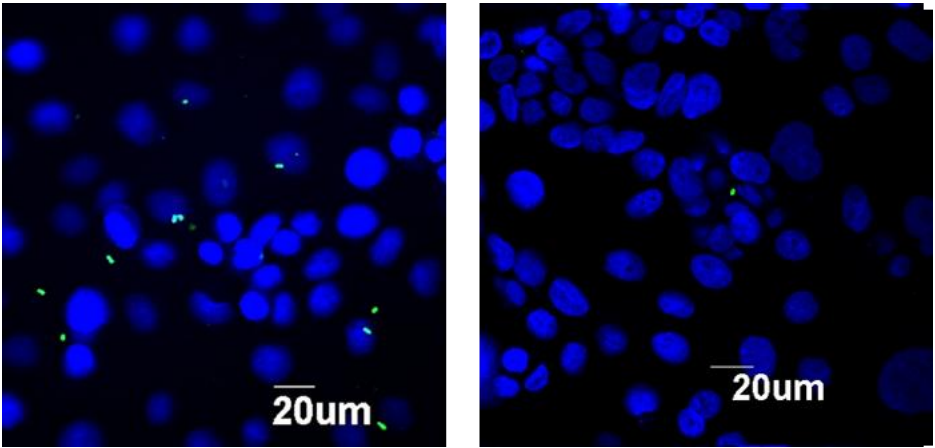
A



B



C



D

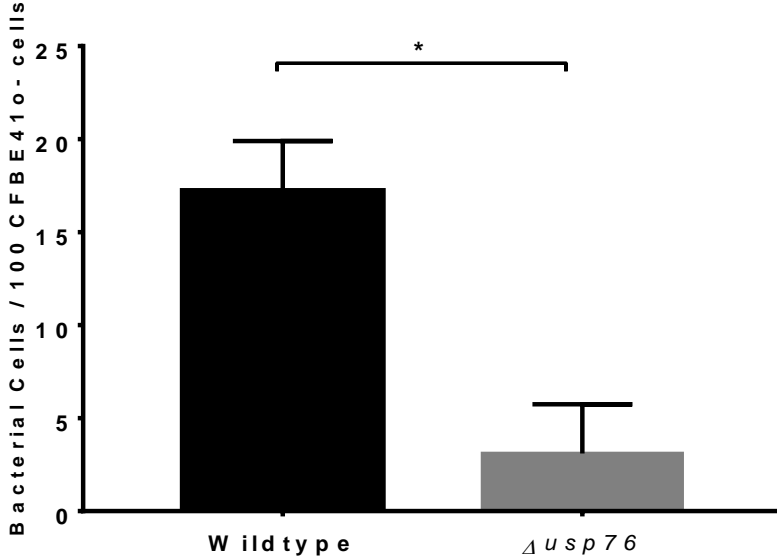
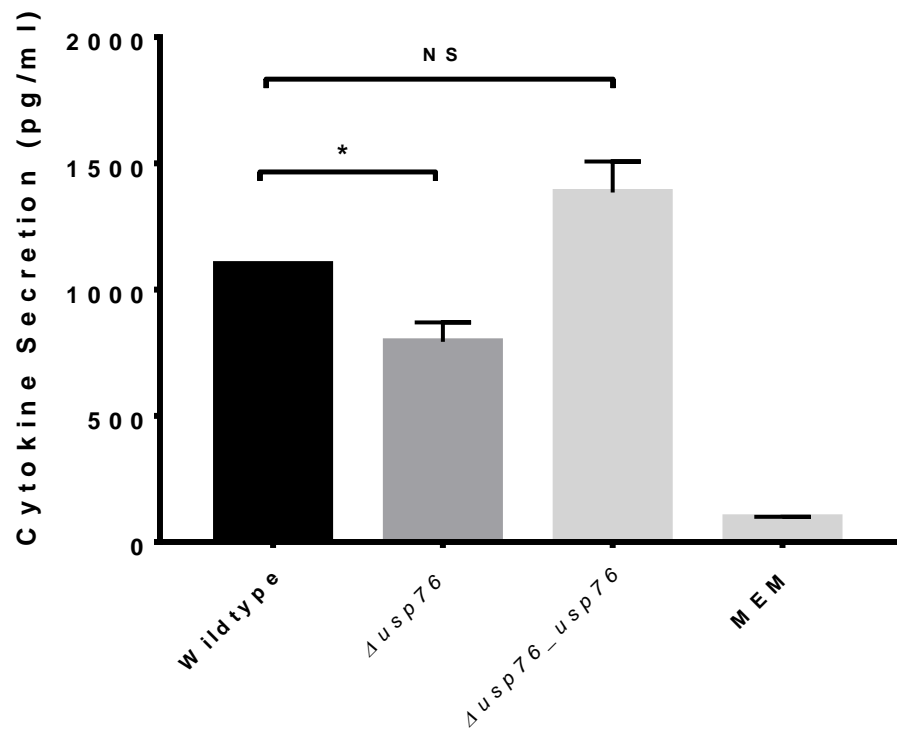


Figure 2

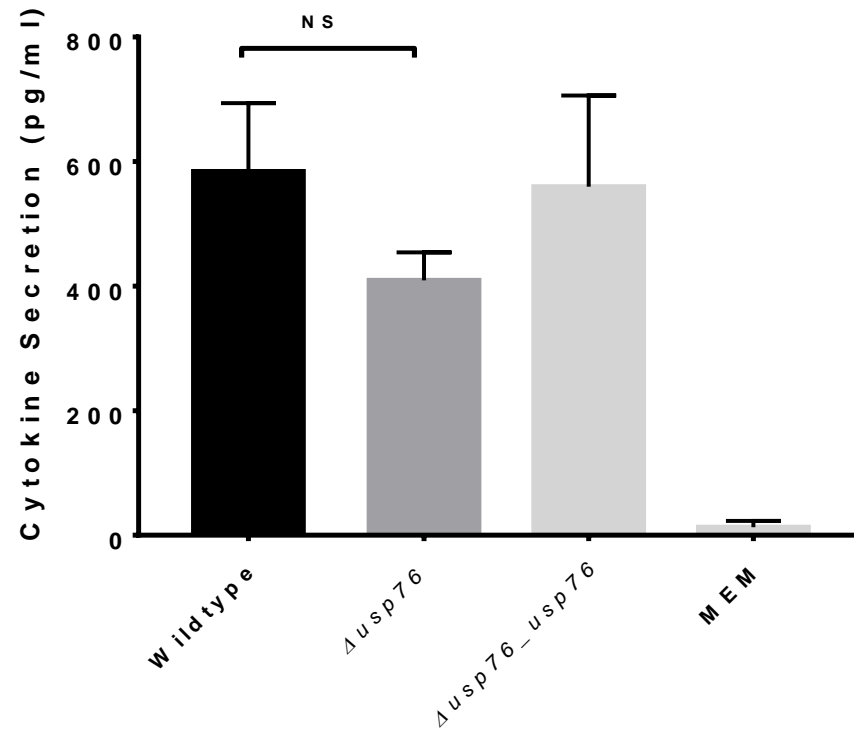
A

IL-8



B

IL-6



C

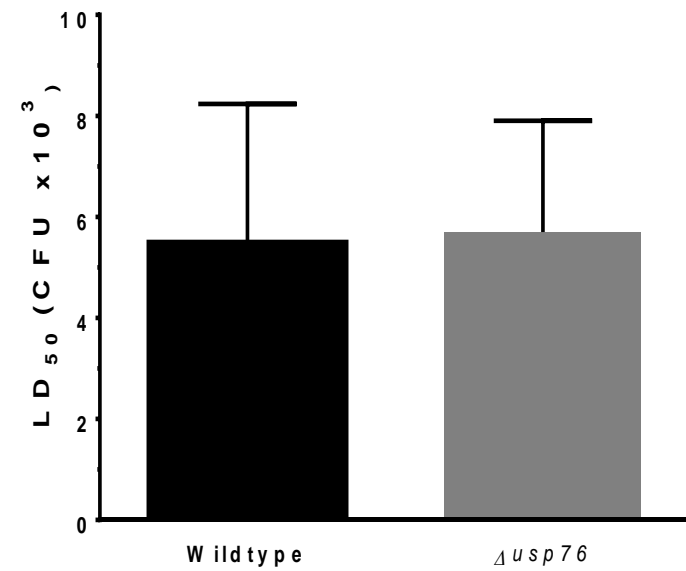
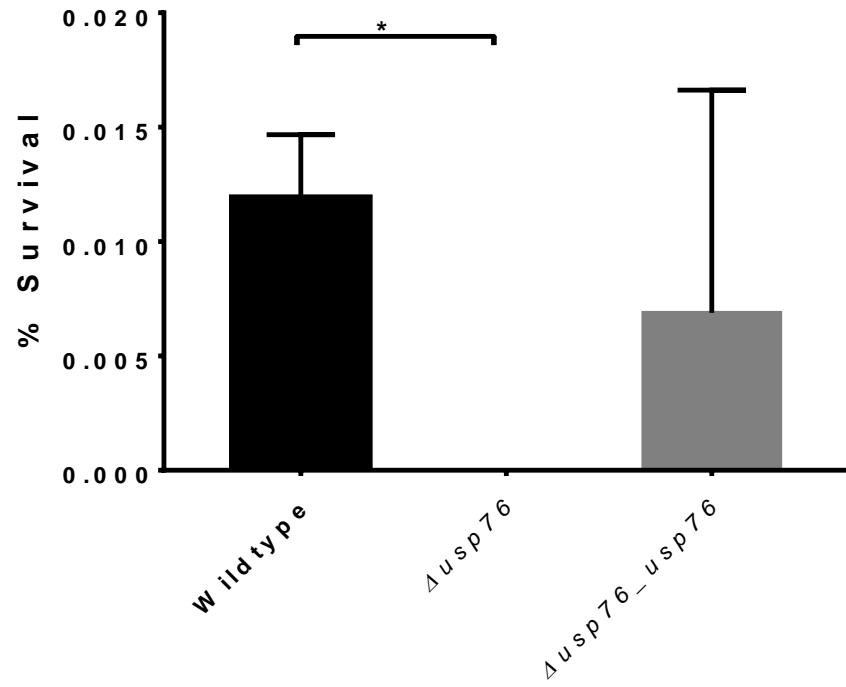
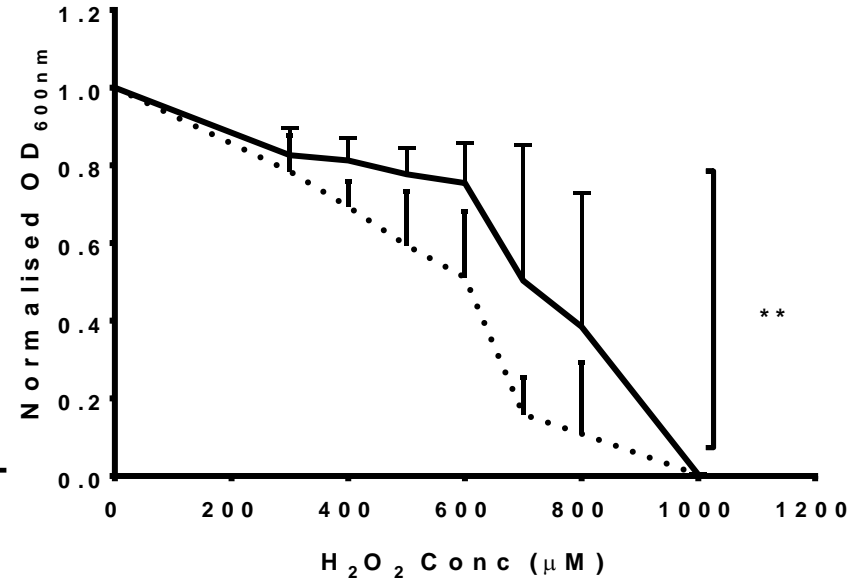


Figure 3

A



B



C

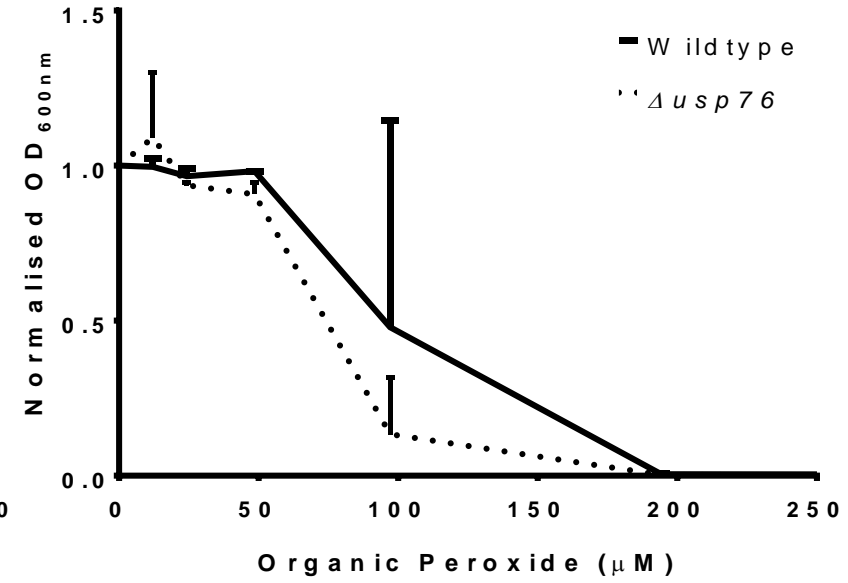
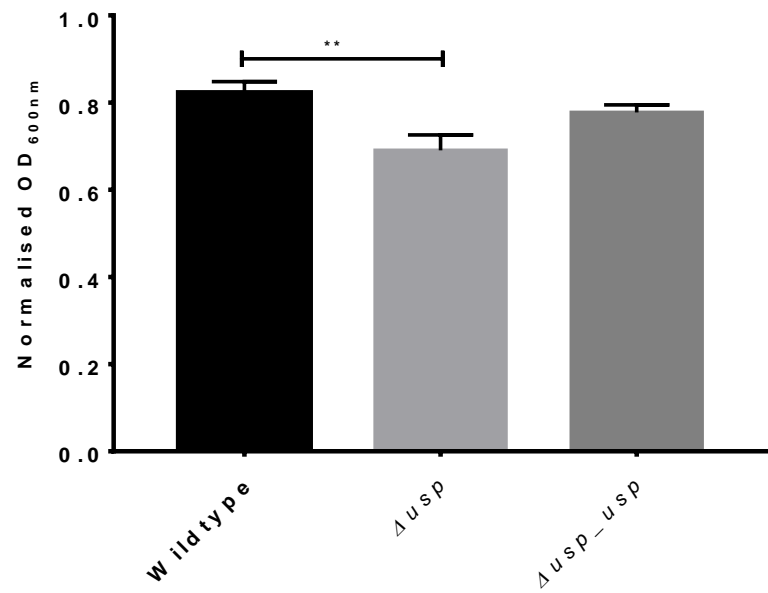
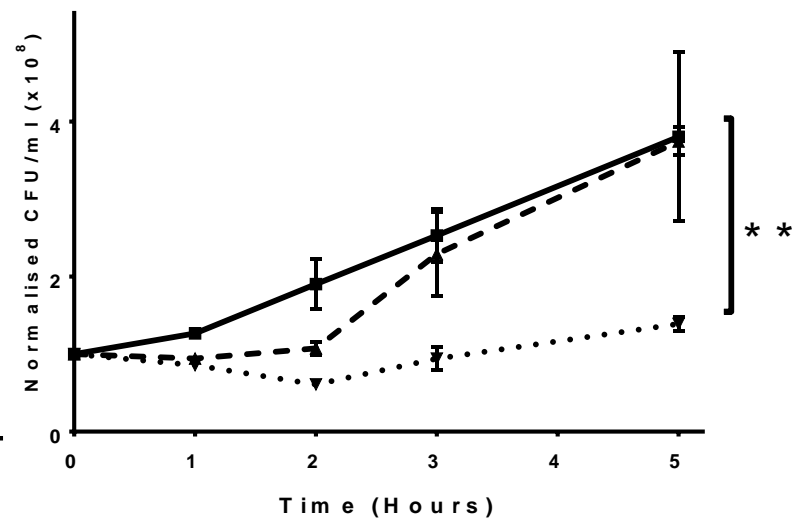


Figure 4

A



B



C

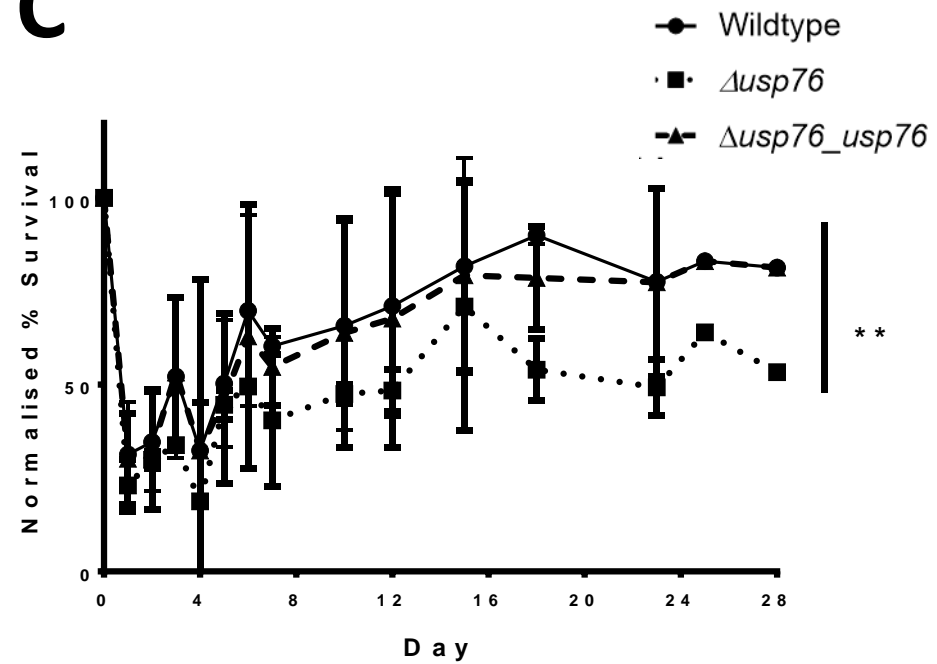
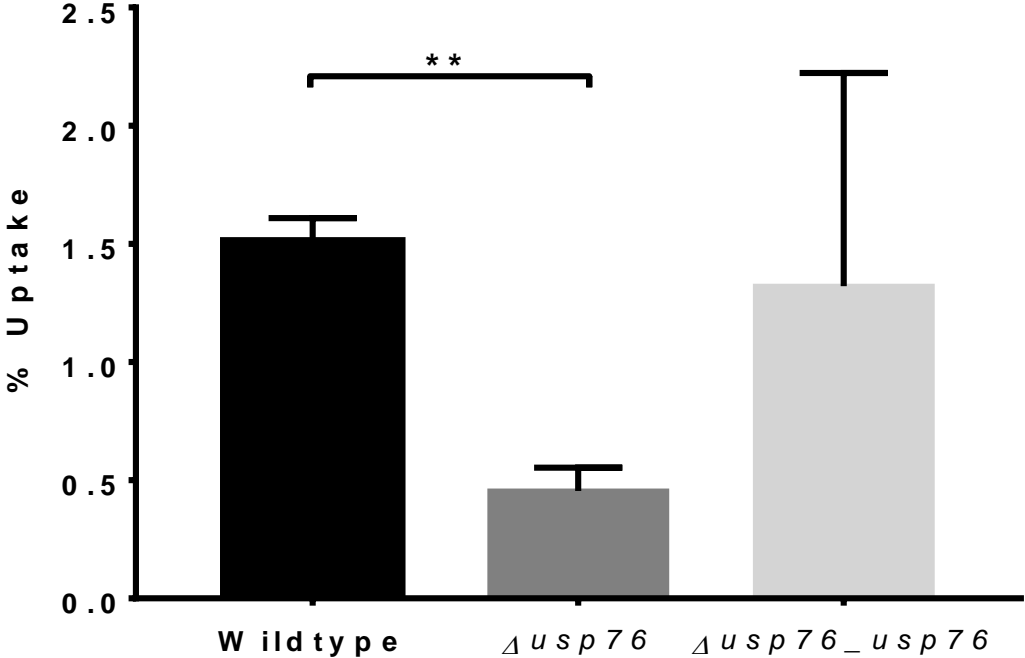


Figure 5

A



B

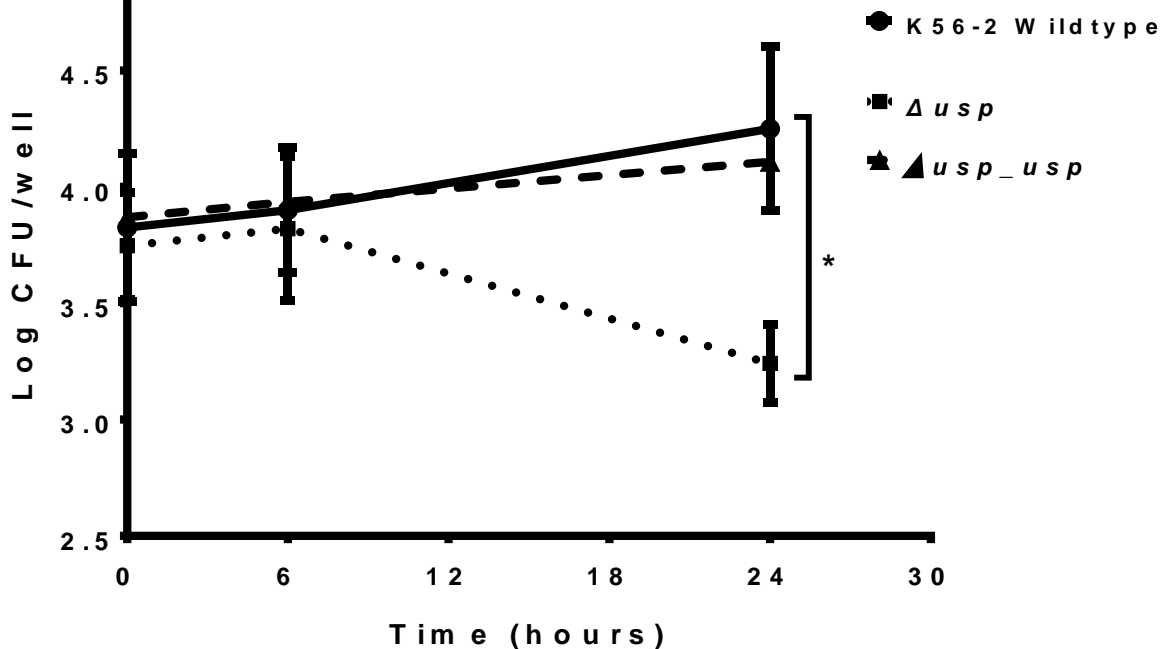
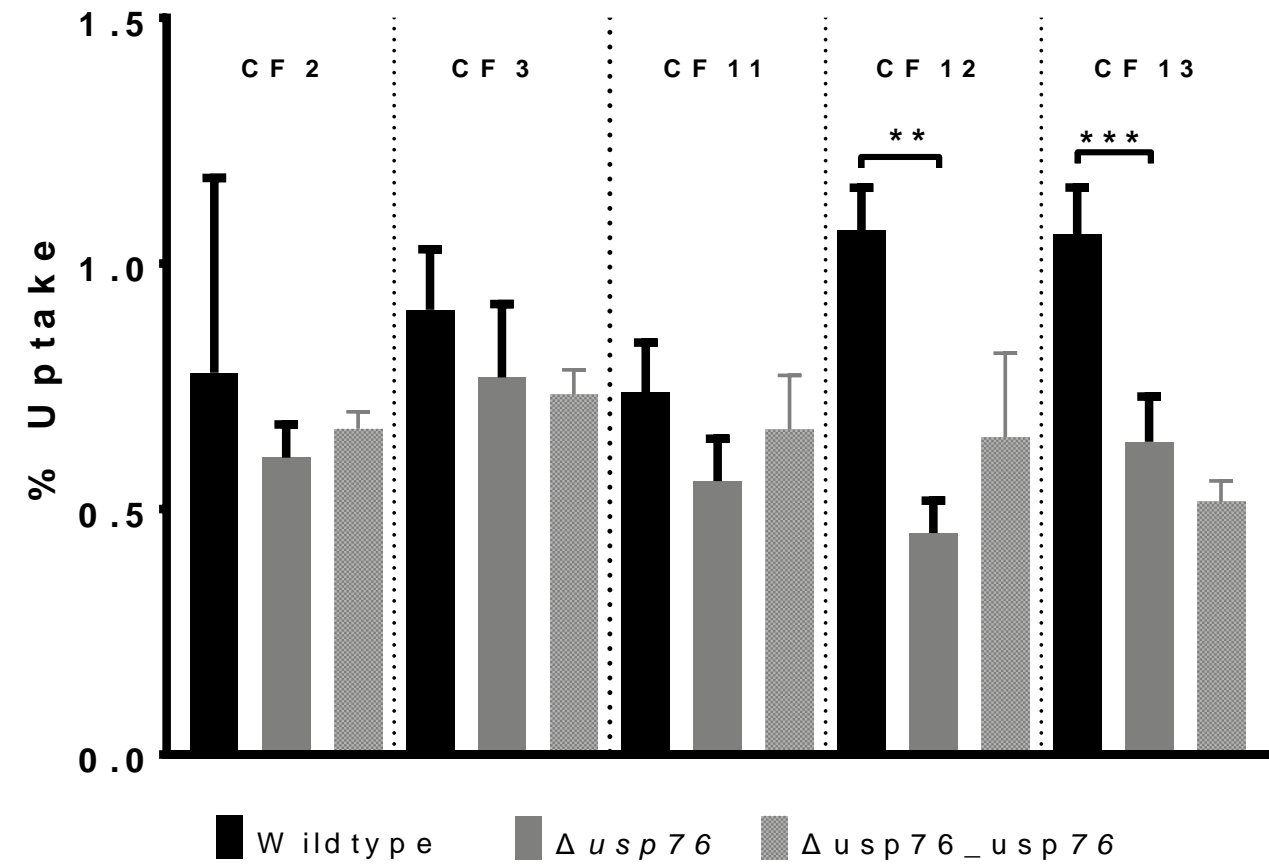


Figure 6.

A



B

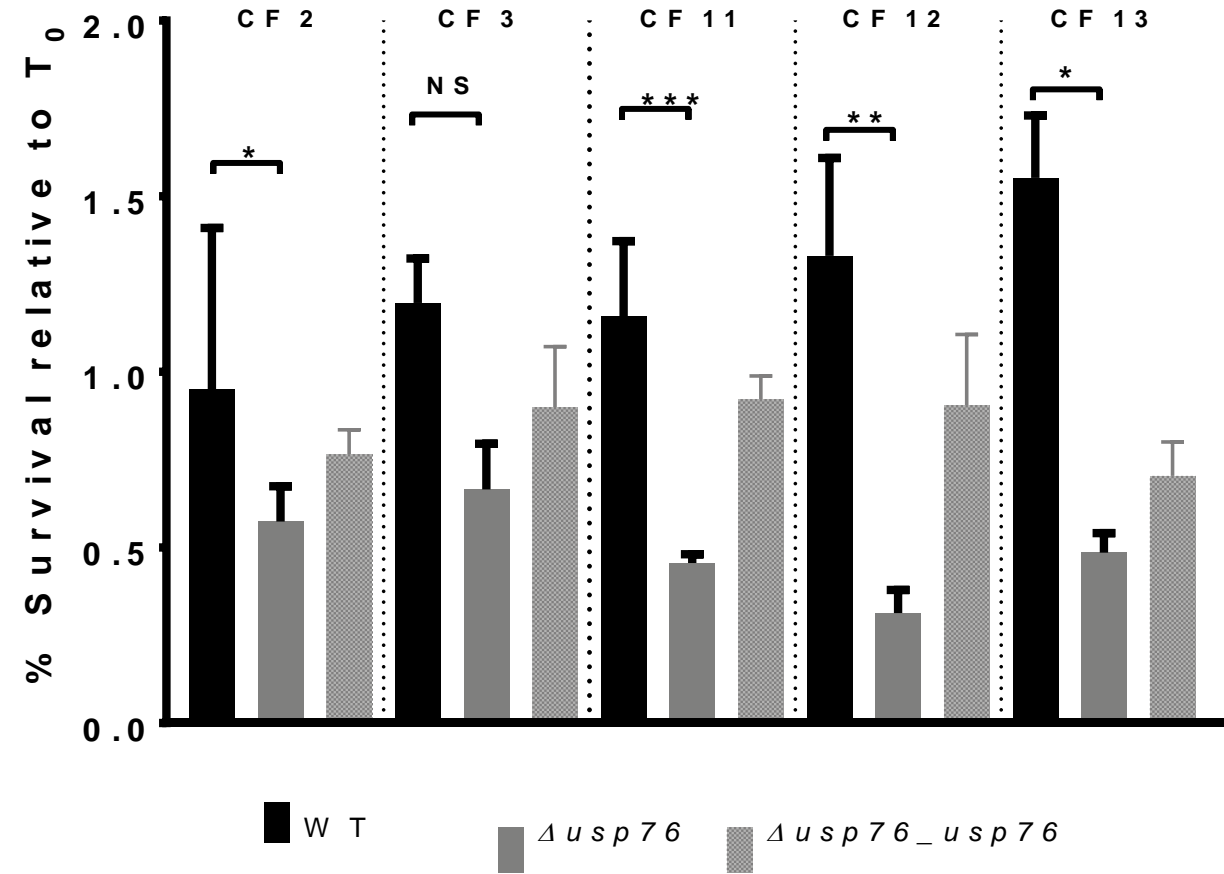


Figure 7

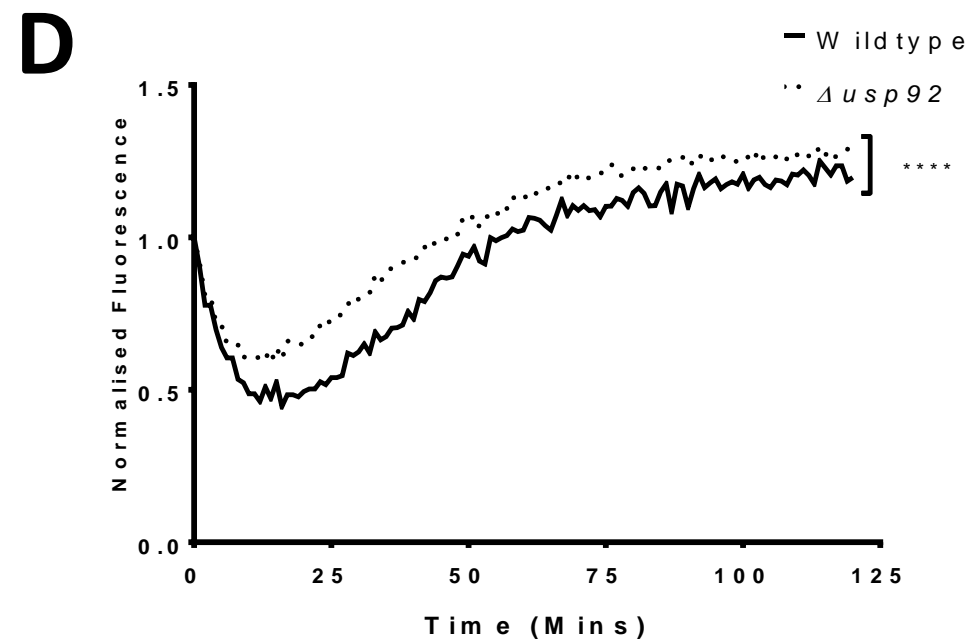
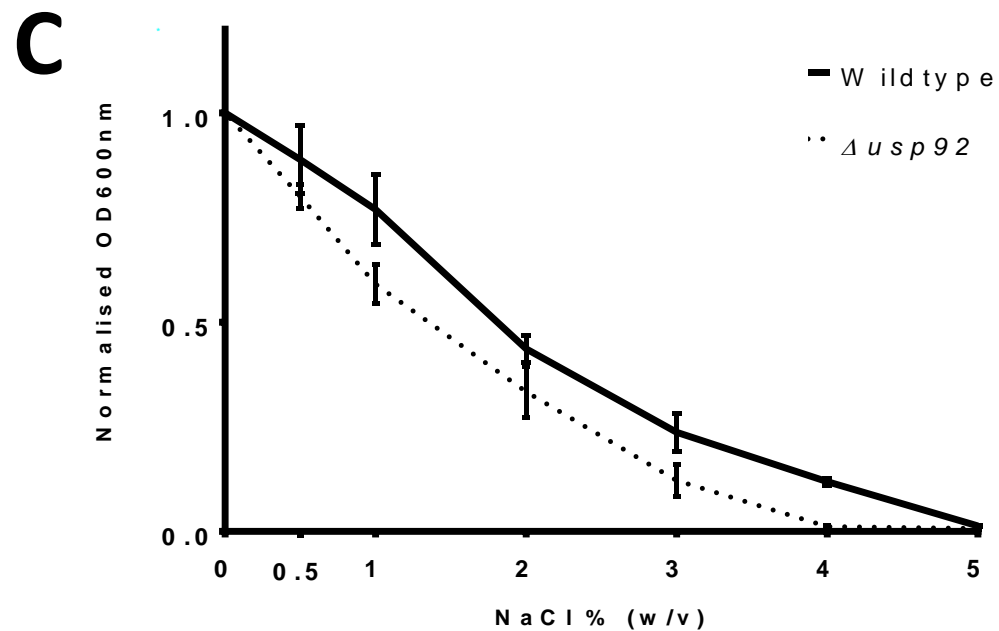
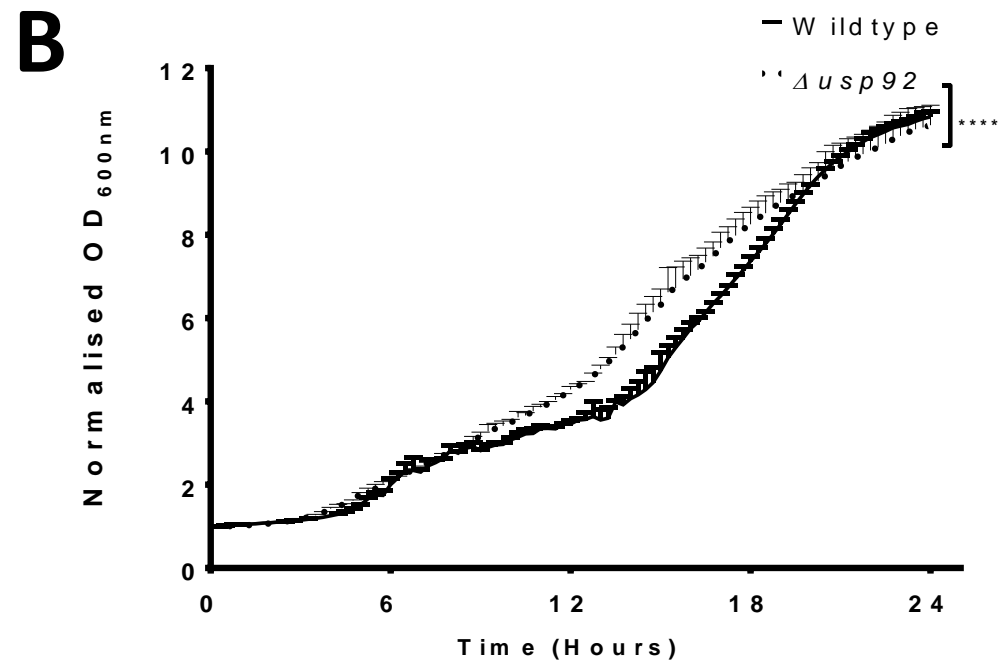
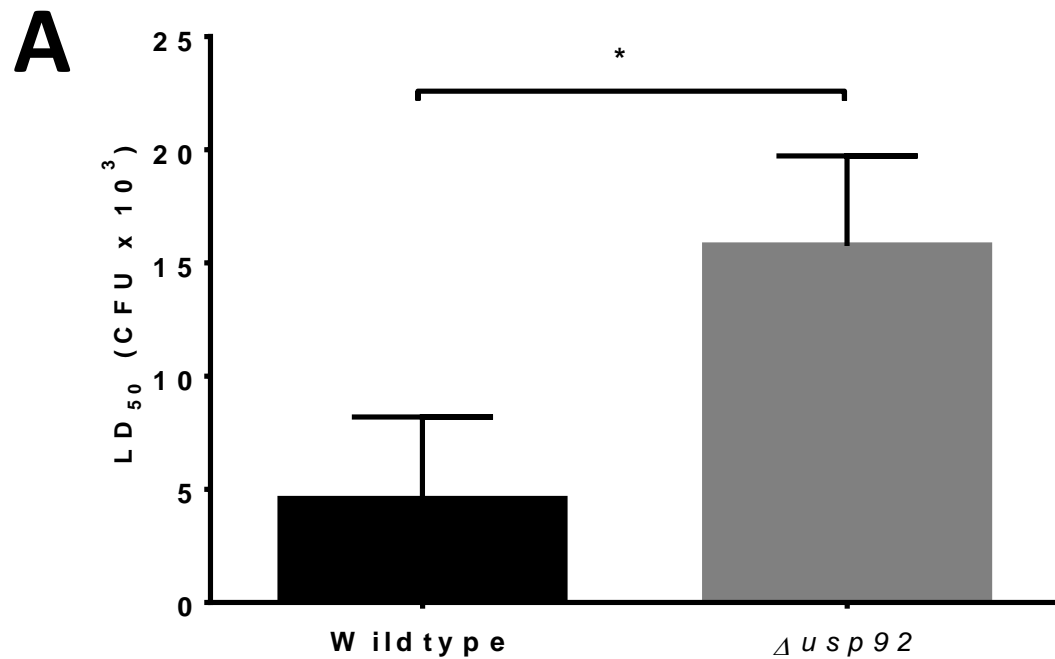


Figure 9

